

EFFECT OF SUBCOOLING ON FILM BOILING
IN A HORIZONTAL TUBE

by

EDWARD FRANCIS DOYLE

B.S., Massachusetts Institute of Technology (1959)

SUBMITTED IN PARTIAL FULFILLMENT
OF THE REQUIREMENTS FOR THE
DEGREE OF MASTER OF
SCIENCE

at the

MASSACHUSETTS INSTITUTE OF
TECHNOLOGY

June, 1962

Signature of Author.....
Department of Mechanical Engineering, May 28, 1962

Certified by.....
Thesis Supervisor

Accepted by.....
Chairman, Departmental Committee
on Graduate Students

EFFECT OF SUBCOOLING ON FILM BOILING
IN A HORIZONTAL TUBE

by

EDWARD F. DOYLE

Submitted to the Department of Mechanical Engineering on May 28, 1962 in partial fulfillment of the requirements for the degree of Master of Science.

ABSTRACT

An analytical and experimental study is presented for stable film boiling of a liquid in forced convection inside a horizontal tube when the entering liquid is subcooled.

Tube wall temperatures were measured for Freon-113 flowing inside an electrically heated stainless steel tube. At the same heat transfer rate and flow rate, higher tube wall temperatures were observed for subcooled liquid flow than for saturated liquid flow. An analytical model is presented describing this effect.

Thesis Supervisor: Warren M. Rohsenow

Title: Professor of Mechanical Engineering

ACKNOWLEDGEMENTS

A grant from the National Science Foundation provided the financial support necessary for the investigation conducted and reported in this thesis.

The completion of this report was greatly aided by the following people. To them I wish to express my sincere thanks for the valuable assistance they rendered.

I am deeply grateful to my thesis advisor, Professor Warren M. Rohsenow, whose guidance and assistance were generously provided throughout the entire program.

Dr. Robert A. Kruger designed the equipment and his investigation of film boiling in horizontal tubes was the basis for this project.

Mr. Richard S. Dougall provided many valuable suggestions and assisted in operating the equipment and in performing the calculations.

My wife, Mary, was particularly helpful throughout the program, especially in the preparation of this report.

TABLE OF CONTENTS

	page
I. Introduction.....	8
II. Theoretical Program.....	11
A. Introduction.....	11
B. Liquid Subcooling Heat Transfer Rate.....	12
C. Heat Transfer Coefficient Across the Thin Vapor Film.....	18
D. Ratio of Vapor Area to Liquid Area at any Cross Section.....	20
E. Heat Transfer Coefficient for the Vapor Layer.....	22
F. Conduction in the Tube Wall.....	24
G. Method of Calculation.....	27
III. Experimental Program.....	29
A. Introduction.....	29
B. Description of Apparatus.....	29
C. Measurements and Accuracy.....	32
D. Experimental Technique.....	34
E. Data Recorded.....	37
IV. Results and Conclusions.....	38
A. Discussion.....	38
B. Summary of Results and Conclusions.....	44
Nomenclature.....	45
Bibliography.....	48

Appendix A Velocity Profile in the Vapor Film..... 50
Table of Experimental Results..... 52
Figures..... 59

TABLE OF FIGURES

	page
Figure 1 - Photograph of Film Boiling in a Horizontal Tube with $V_o = 1.85$ ft/sec.....	59
Figure 2 - Schematic Diagram of the Circulation System.	60
Figure 3 - Schematic Diagram of the Visual Test Section.....	61
Figure 4 - Schematic Diagram of the Quantitative Test Section.....	61
Figure 5 - Photograph of the Apparatus Control Panel...	62
Figure 6 - Photograph of the Quantitative Test Section and parts of the Control and Circulation Systems.....	63
Figure 7 - Cross Section of the Idealized Flow Model...	64
Figure 8 - Geometry for the Momentum Analysis.....	64
Figure 9 - Geometry for the Conduction Analysis.....	64
Figure 10 - Boiling Heat Transfer Coefficient Averaging Factor vs. d/π	65
Figure 11 - Tube Length - Flow Rate Parameter vs. d/π ...	65
Figure 12 - Temperature Distributions for $V_o = 1.85$ ft/sec and $\overline{q/A} = 15420$ Btu/hr-ft ²	66
Figure 13 - Temperature Distributions for $V_o = 1.85$ ft/sec and $\overline{q/A} = 17170$ Btu/hr-ft ²	67
Figure 14 - Temperature Distributions for $V_o = 1.23$ ft/sec and $\overline{q/A} = 17830$ Btu/hr-ft ²	68

Figure 15 - Mean Wall Temperature Distributions for $V_o = 1.85$ ft/sec and $\overline{q/A} = 15250$ Btu/hr-ft ²	69
Figure 16 - Mean Temperature Distributions for $V_o =$ 1.85 ft/sec and $\overline{q/A} = 15420$ Btu/hr-ft ²	70
Figure 17 - Mean Temperature Distributions for $V_o =$ 1.85 ft/sec and $(T_s - T_f) = 15^\circ\text{F}$	71
Figure 18 - Mean Temperature Distributions for $V_o =$ 1.85 ft/sec and $(T_s - T_f) = 20^\circ\text{F}$	72
Figure 19 - Mean Temperature Distributions for $V_o =$ 1.85 ft/sec and $(T_s - T_f) = 25^\circ\text{F}$	73
Figure 20 - Mean Temperature Distributions for $V_o =$ 1.85 ft/sec and $(T_s - T_f) = 30^\circ\text{F}$	74
Figure 21 - Mean Temperature Distributions for $V_o =$ 1.85 ft/sec and $(T_s - T_f) = 35^\circ\text{F}$	75
Figure 22 - Mean Temperature Distributions for $V_o =$ 1.85 ft/sec and $(T_s - T_f) = 48^\circ\text{F}$	76

I INTRODUCTION

In recent years, the process of evaporation has been subjected to careful study. Several distinct regions of boiling exist. The actual process of heat transfer is different in each region. Thorough discussions of the different regions of boiling have been presented by Rohsenow (ref. 1) and Westwater (ref. 2).

When the heating surface is at a temperature only slightly higher than the liquid saturation temperature, the liquid is superheated by natural convection and the heat transferred away at the surface by evaporation.

At somewhat higher values of temperature difference between the heating surface and the liquid, bubbles form at active nuclei on the heated surface and break away. The stirring action of the bubbles in the liquid results in much higher heat transfer rates than that due to natural convection. This nucleate boiling is the type encountered in most commercial applications.

In the transition region which occurs at higher temperature differences, the heat transfer rate drops with increasing temperature difference. Berenson (ref. 3) describes transition boiling as a combination of unstable nucleate and unstable film boiling.

Stable film boiling occurs at very large temperature differences. In film boiling, heat transfer rate again increases with increasing temperature difference. A thin vapor layer prevents the liquid from wetting the heated surface in stable film boiling. Radiation is important in film boiling due to the high temperature differences. Film boiling is the type of boiling that is discussed in this report.

Stable film boiling on external geometries has been observed and treated by several investigators. Bradfield (ref. 4) and Cess and Sparrow (ref. 5) analyzed laminar forced convection film boiling. Bromley discussed film boiling on a horizontal rod in natural convection (ref. 6) and in forced convection (ref. 7), and developed methods for predicting the heat transfer rates.

On vertical surfaces, Hsu and Westwater (ref. 8) found the film boiling coefficients were higher than those predicted by Bromley's laminar boundary layer analysis and explained the difference as resulting from turbulence in the boundary layer (ref. 9).

Graham (ref. 10) and von Glahn (ref. 11) investigated film boiling of cryogenic fluids inside vertical tubes.

Film boiling in horizontal tubes in forced convection without liquid subcooling was investigated by Kruger (ref. 12). He developed a method of predicting tube wall temperature distribution for constant heat transfer rates along the tube.

The purpose of this investigation was to study the effect of liquid subcooling on film boiling in horizontal tubes. This is a direct extension of the investigation conducted by Kruger.

In a horizontal tube, the vapor produced travels up the side of the tube in a thin film and collects at the top of the tube forming a stratified flow which increases in thickness as it travels down the tube. The nature of the flow can be seen in Figure 1, and the flow model as developed by Kruger is shown in Figures 7 through 9.

The object of the theoretical program was to extend the analysis by Kruger to include the effect of subcooling in the method for calculating tube wall temperatures for a given flow rate and heat transfer rate. Motte and Bromley (ref. 13) derived a relationship for film boiling of flowing subcooled liquids. However, it was not sufficiently similar to this case to be applied.

The object of the experimental program was to relate the tube wall temperature distribution to the heat transfer rate, flow velocity, and liquid subcooling. Only minor changes in the apparatus originally designed by Kruger were necessary for this program.

Both the theoretical and experimental programs reported here and by Kruger are limited to the case where the mass flow of vapor is small compared to the total mass flow in the tube.

II THEORETICAL PROGRAM

A. Introduction

The object of the theoretical program was to include the effect of subcooling of the liquid in the analysis of film boiling in a horizontal tube as developed by Kruger (ref. 12). The analysis is limited to the case of constant heat transfer rate along the tube and to the region in which the mass flow of vapor at the tube outlet is small compared to the total mass flow.

Visual observation of the flow showed that subcooling the liquid had no effect on the basic stratified flow pattern. The flow model, shown in Figures 7 through 9, remains the same as developed by Kruger. Vapor is formed in a thin film at the hot tube wall preventing the liquid from wetting the surface. Under the action of buoyancy forces, the vapor flows upward along the hot tube wall and collects in a vapor layer that flows along the top of the tube. The range in which this stratified flow model applies has not been determined.

Subcooling reduces the rate of vapor formation, and this effect must be introduced into the relations developed by Kruger. The exact nature of the subcooling process must be defined to determine the magnitude of this effect.

In order to determine the tube wall temperature distribution for a given heat transfer rate, flow velocity, and initial

liquid subcooling, five basic relations are combined. These relations are for the liquid subcooling heat transfer rate, heat transfer coefficient across the thin vapor film, the vapor layer heat transfer coefficient, the ratio of vapor area to liquid area at any cross section, and conduction around the tube wall.

B. Liquid Subcooling Heat Transfer Rate

In order to determine the subcooling heat transfer rate, the liquid flow must be examined. Since the liquid is completely surrounded by vapor, the shearing forces on the liquid surface are entirely different than for a liquid flowing through a tube.

The vapor effectively lubricates the tube wall so that the liquid slips along the tube. In the absence of opposing shearing forces, the liquid would essentially have a uniform velocity profile in the flow direction. Actually, the vapor layer at the top of the tube, which moves faster than the liquid, tends to increase the liquid flow rate along the tube. The vapor flowing upward along the tube tends to introduce a secondary flow in the liquid. In this secondary flow the liquid at the vapor film interface moves upward along the vapor film and then mixes in the liquid core.

The relative liquid velocity with respect to vapor velocity at the interface is much lower than the absolute liquid velocity for both the main flow along the tube and for the secondary flow at the vapor film. For the liquid flow

velocities encountered in the experiment, turbulent flow would result if the liquid did not have a vapor layer around it. However, with the vapor layer, a laminar liquid flow could exist.

The controlling subcooling heat transfer mechanism could be either the main liquid flow down the tube or the secondary flow along the vapor film. Both cases were considered. The criterion to determine the more important mechanism is the ratio of tube length divided by axial liquid velocity (L/V_0) to the tube diameter divided by liquid interface velocity (D/L_{VF}). This determines the time of boundary layer development in the liquid flow.

To evaluate this ratio, the liquid interface velocity must be determined. One method to determine this is from the factor β' as defined by Kruger (ref. 12) and discussed in Appendix A. Kruger experimentally determined a value of 1.4 for β' . As shown in Appendix A, this corresponds to a value of liquid interface velocity equal to 1.085 times the average vapor velocity in the film. For the values encountered in the experiment, D/L_{VF} would be much greater than L/V_0 indicating that the secondary flow is the important heat transfer mechanism. However, other considerations indicate that this may not be true. First, the value of β' might be misleading since it is experimentally determined and could include effects not considered in the theory. Secondly, use of this value of β' leads to values of subcooling heat transfer rates much higher than

encountered in the experiment. As discussed in more detail in the section on experimental results, another effect was encountered in the experiment which indicates that the primary flow rather than the secondary flow might be the more important mechanism. With liquid subcooling, the tube wall temperatures near the tube outlet unexpectedly exceeded the highest temperature encountered anywhere on the tube for a saturated liquid flow. As much as 100°F higher tube wall temperatures were encountered for 50°F of subcooling.

A simple calculation shows that, for the heat transfer rates and flow rates encountered in the experiments, a liquid subcooled 50°F will not rise greatly in temperature. This is an important consideration. If the secondary flow was the main subcooling heat transfer mechanism, the resulting heat transfer coefficient would be approximately constant along the length of the tube. With the amount of subcooling remaining constant over the length of the tube, the subcooling heat transfer rate would be approximately constant. When this effect is combined with the other relationships, the tube wall temperature is always lower with subcooling than for the corresponding case for saturated liquid.

When the primary liquid flow is considered as the controlling subcooling heat transfer mechanism, the heat transfer coefficient decreases along the tube and the subcooling heat transfer rate also decreases. This effect, when combined with

the other relationships, can result in the higher tube wall temperatures observed with subcooling.

Since the liquid interface velocity could not be accurately determined, and since the experiment indicated that the primary flow might be the controlling subcooling mechanism, the primary flow is considered as controlling in the theory. The effect of the secondary flow will be neglected.

If a uniform velocity profile is assumed for the primary liquid flow along the tube, the liquid can be considered as a semi-infinite solid of uniform temperature, T_f . At the tube entrance, it is exposed to a constant surface temperature, T_s , equal to the saturation temperature. The liquid bulk temperature, T_f , will be considered constant along the tube. The energy equation for this model is

$$\rho_L c_{pL} \frac{dT_L}{dt} = k_L \frac{d^2 T_L}{dy^2} \quad (\text{II-1})$$

where T_L is the liquid temperature, y the distance from the liquid vapor interface inward, and t the time.

For constant fluid properties and for constant surface temperature, T_s , applied at $y = 0$ and $t = 0$, the solution of equation (II-1) is given by (ref. 14)

$$\frac{T_L - T_s}{T_f - T_s} = \text{erf} \frac{y}{2\sqrt{\left(\frac{k}{\rho c_p}\right)_L t}} \quad (\text{II-2})$$

where erf is the error function.

The subcooling heat transfer rate per unit area is given by

$$q/A_{sc} = -k_L \left(\frac{dT_L}{dy} \right)_{y=0} = -k_L (T_s - T_f) \frac{1}{\sqrt{\pi}} \sqrt{\left(\frac{\rho c_p}{k}\right)_L} \sqrt{\frac{1}{t}} \quad (\text{II-3})$$

The time in equation (II-3) is the time required for the liquid to travel from the entrance to a position x along the tube. This is given by

$$t = \frac{x}{\bar{V}_L} \quad (\text{II-4})$$

where \bar{V}_L is the average liquid velocity to the position x .

The liquid velocity V_L is

$$V_L = \frac{w_L}{\rho_L A_L} \quad (\text{II-5})$$

Since the mass of vapor formed is small compared to the total mass flow, w_L is considered constant. The liquid area can be written as

$$A_L = \frac{\pi D^2}{4} \left[1 - \frac{\alpha}{\pi} + \frac{1}{2\pi} \sin 2\alpha \right] \quad (\text{II-6})$$

where D is the tube diameter and the angle α is defined in Figure 7.

At the tube entrance

$$w_L = \rho_L V_0 \frac{\pi D^2}{4} \quad (\text{II-7})$$

Combining these equations

$$V_L = \frac{V_0}{\left[1 - \frac{\alpha}{\pi} + \frac{1}{2\pi} \sin 2\alpha \right]} \quad (\text{II-8})$$

and

$$\bar{V}_L = \int_0^x \frac{V_0 dx}{\left[1 - \frac{\alpha}{\pi} + \frac{1}{2\pi} \sin 2\alpha \right]} \quad (\text{II-9})$$

Combining this relation with (II-3)

$$\bar{q}/A_{sc} = \frac{k(T_s - T_f)}{\sqrt{\pi}} \left(\frac{\rho c_p}{k} \right)_L^{1/2} \sqrt{\frac{V_0}{x}} \int_0^x \frac{dx}{\sqrt{1 - \frac{\alpha}{\pi} + \frac{1}{2\pi} \sin 2\alpha}} \quad (\text{II-10})$$

This heat transfer rate is based on the liquid surface area given by

$$dA_{LS} = \pi D \left(1 - \frac{\alpha}{\pi} + \frac{1}{\pi} \sin 2\alpha \right) dx \quad (\text{II-11})$$

Introducing this relation

$$\frac{\bar{q}_{sc}}{\pi D} = \frac{k(T_s - T_f)}{\sqrt{\pi}} \sqrt{\frac{V_0}{x}} \left(\frac{\rho c_p}{k} \right)_L^{1/2} \int_0^x \frac{dx}{\left(1 - \frac{\alpha}{\pi} + \frac{1}{2\pi} \sin 2\alpha \right)} \int_0^x \left(1 - \frac{\alpha}{\pi} + \frac{\sin \alpha}{\pi} \right) dx \quad (\text{II-12})$$

$\bar{q}_{sc}/\pi D$ is the average subcooling heat transfer rate based on the tube area, \bar{q}/A_{sc} .

For $0 \leq \frac{\alpha}{\pi} \leq .50$ the combined integrals in equation (II-12) are always approximately equal to 1.0 making this simplification

$$\bar{q}/A_{sc} = \frac{k(T_s - T_f)}{\sqrt{\pi}} \left(\frac{\rho c_p}{k} \right)_L^{1/2} \sqrt{\frac{V_0}{x}} \quad (\text{II-13})$$

From equation (II-13) the assumption of a constant liquid bulk temperature, T_f , can be verified. For the range of the experiment T_f increases a maximum of 10% at the tube outlet.

Relation (II-13) can also be written as

$$\bar{q}/A_{sc} = \frac{k}{\sqrt{\pi}} (T_s - T_f) \left(\frac{\mu c_p}{k} \right)_L^{1/2} \sqrt{\frac{\rho V_0}{\mu x}} \quad (\text{II-14})$$

This is the same relation obtained by considering a uniform velocity profile in the boundary layer over a flat plate.

The local average value of subcooled heat transfer is given by

$$\overline{q/A_{scL}} = \frac{1}{\pi D} \frac{d}{dx} (q/A_{sc} \pi D x) = \frac{1}{2} \overline{q/A_{sc}} \quad (\text{II-15})$$

and then basing the local value on the liquid surface area

$$\overline{q/A_{scL}} = \frac{\frac{1}{2} \overline{q/A_{sc}}}{\left(1 - \frac{\alpha}{\pi} + \frac{1}{\pi} \sin \alpha\right)} \quad (\text{II-16})$$

In considering the secondary flow, equation (II-3) can be used, but in this case, t equals the distance the liquid travels upward along the vapor film divided by the average liquid interface velocity. Since this effect is not considered as controlling, the complete derivation is not presented.

C. Heat Transfer Coefficient Across the Thin Vapor Film

Subcooling reduces vapor formation, and the equations developed by Kruger (ref. 12) must be revised to include this effect. Heat flows into the liquid vapor interface from the hot tube wall by radiation and convection while heat is removed from the interface by convection into the subcooled liquid. The rate of vapor formation per unit area at the vapor film interface is given by

$$\frac{dw_{VF}}{d\theta} = \frac{D(q/A_T - q/A_{scL})}{2\gamma'_{VF}} \quad (\text{II-17})$$

where q/A_T is the heat transfer rate from the tube wall by both radiation and convection in the vapor film region, q/A_{scL} is the subcooling heat transfer locally, and λ'_{VF} is the average heat content of the vapor in the film above that of saturated liquid.

Assuming laminar flow in the vapor film and neglecting momentum changes, the following equations can be written for the geometry shown in Figure 7.

For control volume A

$$\frac{dp}{d\theta} = -\rho_L g \frac{D}{2} \sin \theta \quad (\text{II-18a})$$

For control volume B

$$\frac{dp}{d\theta} = -\rho_V g \frac{D}{2} \sin \theta - \tau_{WT} \frac{D}{2b} \quad (\text{II-18b})$$

The total shearing stress on the vapor, τ_{WT} , can be written as (see Appendix A)

$$\tau_{WT} = 2(\beta')^3 \frac{\mu_V w_{VF}}{\rho_V b^2} \quad (\text{II-19})$$

where as shown by Kruger (ref. 12) and as derived in Appendix

$$A \quad 3/2 \leq (\beta')^3 \leq 6 \quad (\text{II-20})$$

These two extremes represent the cases where the liquid is either completely rigid or completely frictionless.

Combining (II-18a), (II-18b), and (II-19), the vapor film thickness, b , can be obtained.

$$b = \beta' \left\{ \frac{\mu_V [(\rho/A)_T - (\rho/A)_{scL}] D}{\rho_V (\rho_L - \rho_V) g \lambda'_{VF}} \right\}^{1/3} \left\{ \frac{\theta}{\sin \theta} \right\}^{1/3} \quad (\text{II-21})$$

Assuming a linear temperature distribution in the vapor, the local boiling heat transfer coefficient can be written as

$$h_{LB} = K/b \quad (\text{II-22})$$

Combining (II-21) and (II-22)

$$h_{LB} = \frac{1}{\beta'} \left\{ \frac{\kappa_V^3 \rho_V (\rho_L - \rho_V) g \lambda'_{VF}}{D \mu_V (g/A_T - g/A_{scL})} \right\}^{1/3} \left\{ \frac{\sin \theta}{\theta} \right\}^{1/3} \quad (\text{II-23})$$

The average heat transfer coefficient in the boiling region is

$$\bar{h}_{LB} = \frac{1}{\pi - \alpha} \int_0^{\pi - \alpha} h_{LB} d\theta \quad (\text{II-24})$$

defining

$$\gamma \equiv \frac{1}{\pi - \alpha} \int_0^{\pi - \alpha} \left(\frac{\sin \theta}{\theta} \right)^{1/3} d\theta \quad (\text{II-25})$$

The average coefficient can be written as

$$\bar{h}_{LB} = \frac{\gamma}{\beta'} \left\{ \frac{\kappa_V^3 \rho_V (\rho_L - \rho_V) g \lambda'_{VF}}{D \mu_V (g/A_T - g/A_{scL})} \right\}^{1/3} \quad (\text{II-26})$$

Kruger obtained γ by numerical integration and the result is presented in Figure 10 as a function of α/π . Kruger also determined experimentally that $\beta' = 1.4$.

The properties are evaluated at the mean film temperature. Kruger states that this introduces an error of less than 10%. Evaluation of the properties at this temperature is equally valid with subcooling. The average vapor heat content λ'_{VF} is

$$\lambda'_{VF} = \lambda + \frac{1}{2} C_{pV} (T_w - T_s) \quad (\text{II-27})$$

D. Ratio of Vapor Area to Liquid Area at Any Cross Section

The ratio of vapor area to liquid area at any cross section can be obtained by applying the momentum equation to the control volumes shown in Figure 8.

For control volume A

$$\left(\frac{dP}{dx} \right)_V A_V - \tau_i D \sin \alpha - \tau_{wV} \alpha D = \frac{d}{dx} (w_{vb} V_V) - V_L \frac{dw_{vb}}{dx} \quad (\text{II-28})$$

For control volume B

$$\left(\frac{\partial p}{\partial x}\right)_L A_L - \tau_{wL} (\pi - \alpha) D + \tau_i D \sin \alpha = \frac{d}{dx} (w_L V_L) + V_L \frac{dw_{vb}}{dx} \quad (\text{II-29})$$

When the mass flow of vapor is small compared to the total mass flow, the above equations can be greatly simplified. With this assumption, Kruger showed that all the frictional terms could be neglected, and that only the momentum change in the liquid, due to the area change, and the momentum change in the vapor, due to the addition of vapor, were important.

The vapor velocity, V_V , liquid velocity, V_L , and vapor area, A_V , can be eliminated from (II-28) and (II-29) with the following equations.

$$V_L = \frac{w_L}{\rho_L A_L} \quad (\text{II-30a})$$

$$V_V = \frac{w_{vb}}{\rho_V A_V} \quad (\text{II-30b})$$

$$A_V = A_T - A_L \quad (\text{II-30c})$$

The pressure gradient in the vapor must equal the pressure gradient in the liquid to maintain continuity of pressure across the horizontal interface. The above equations then

yield

$$\frac{(A_T - A_L)^2}{A_L^3} \frac{\partial A_L}{\partial x} = - \frac{2 \rho_L w_{vb}}{\rho_V w_L^2} \frac{dw_{vb}}{dx} \quad (\text{II-31})$$

The liquid flow rate can be considered constant as given by (II-7).

The vapor flow is

$$w_{vb} = \frac{(\bar{q}TA - \bar{q}/A_{sc}) \pi D x}{\tau_{vb}'} \quad (\text{II-32})$$

where the average heat content of the vapor, λ'_{vb} , is

$$\lambda'_{vb} = \lambda_{vb} + C_{p_{vb}} (T_{vb} - T_s) \quad (\text{II-33})$$

The average subcooling heat transfer rate, $\overline{q/A_{sc}}$, is given by (II-13).

Since w_{vb} is a function of x only (II-31) can be integrated from 0 to x .

$$\left\{ \left(\frac{A_T}{A_L} \right)^2 - 4 \frac{A_T}{A_L} + 2 \ln \frac{A_T}{A_L} + 3 \right\} = \frac{3\rho_L}{\rho_V} \frac{w_{vb}^2}{w_L^2} \quad (\text{II-34})$$

$\frac{A_L}{A_T}$ can be obtained from (II-6).

$$\frac{A_L}{A_T} = 1 - \frac{\alpha}{\pi} + \frac{1}{2\pi} \sin 2\alpha \quad (\text{II-35})$$

defining

$$\underline{X}_M \equiv \sqrt{\frac{3\rho_L}{\rho_V}} \frac{w_{vb}}{w_L} \quad (\text{II-36})$$

combining the above relations

$$\underline{X}_M = \frac{4\sqrt{2} (\bar{q}/A - \bar{q}/A_{sc}) x}{v_L \rho_V v_0 \lambda'_{vb} D} = f\left(\frac{\alpha}{\pi}\right) \quad (\text{II-37})$$

This function is shown in Figure 11.

E. Heat Transfer Coefficient for the Vapor Layer

In order to estimate the heat transferred directly to the vapor layer from the top of the tube, equations for flow in a round tube are used. The concept of hydraulic diameter is introduced to account for the different flow geometry.

For the range of the experiments, the vapor Reynolds number indicates that both laminar and turbulent flows can occur. For this reason, both types of flow must be considered.

The hydraulic diameter is defined by

$$D_e = 4 \frac{\text{cross sectional area}}{\text{wetted perimeter}} \quad (\text{II-38})$$

For the geometry of Figure 7

$$D_e = D \left\{ \frac{d/\pi - \frac{1}{2\pi} \sin 2\alpha}{d/\pi + \frac{1}{\pi} \sin \alpha} \right\} \quad (\text{II-39})$$

For fully developed laminar flow and constant heat transfer rate (ref. 15)

$$\frac{h_{LV} D_e}{K_{vb}} = 4.36 \quad (\text{II-40})$$

Then for laminar flow in the vapor layer, the heat transfer coefficient is

$$h_{LV} = \frac{4.36 K_{vb}}{D} \left\{ \frac{d/\pi + \frac{1}{\pi} \sin \alpha}{d/\pi - \frac{1}{2\pi} \sin 2\alpha} \right\} \quad (\text{II-41})$$

For fully developed turbulent flow (ref. 16)

$$\frac{h_{LV} D_e}{K_{vb}} = .023 \left(\frac{\rho_{vb} V_{vb} D_e}{\mu_{vb}} \right)^{.8} \left(\frac{\mu_{cp}}{K} \right)_{vb}^{.40} \quad (\text{II-42})$$

Using (II-30b), (II-30c), (II-32) and (II-6)

$$V_{vb} = \frac{4(\bar{g}/A - \bar{g}/A_{sc})x}{\rho_{vb} \tau'_{vb} D \left(\frac{d}{\pi} - \frac{1}{2\pi} \sin 2\alpha \right)} \quad (\text{II-43})$$

Then for turbulent flow in the vapor layer, the heat transfer coefficient is

$$h_{LV} = .023 \frac{K_{vb}}{D} \left(\frac{4(\bar{g}/A - \bar{g}/A_{sc})x}{\rho_{vb} \tau'_{vb} D \left(\frac{d}{\pi} - \frac{1}{2\pi} \sin 2\alpha \right)} \right)^{.8} \left(\frac{\mu_{cp}}{K} \right)_{vb}^{.4} \left(\frac{d/\pi + \frac{1}{\pi} \sin \alpha}{d/\pi - \frac{1}{2\pi} \sin 2\alpha} \right)^{.20} \quad (\text{II-44})$$

In order to evaluate the film coefficient, the bulk temperature in the vapor layer must be determined. By using the condition at the horizontal liquid-vapor interface, an analysis was performed to obtain the bulk temperature in the

vapor layer. Calculations indicated that the bulk temperature was approximately half way between the tube wall temperature and the saturation temperature for both saturated and subcooled liquid flows. Using this approximation greatly simplifies the analysis.

The vapor flow is laminar near the tube inlet. At some point along the tube the flow becomes turbulent. The experiments strongly indicate that the transition from laminar to turbulent flow occurs at different vapor Reynolds numbers, depending on the amount of subcooling. With a saturated liquid flow, the experiment indicates the vapor quickly becomes turbulent. With subcooling, the flow appears to remain laminar at higher vapor Reynolds numbers.

At present, no method has been developed for determining the transition vapor Reynolds number as a function of subcooling. For this reason, the flow is assumed turbulent for saturated liquid flows and laminar for highly subcooled flows. No correlation has been determined for intermediate amounts of subcooling.

F. Conduction in the Tube Wall

By using the model shown in Figure 9, Kruger developed an equation for the conduction around the tube. This relation is necessary because the heat transferred into the vapor film at the bottom of the tube can be significantly different from the heat transferred directly to the vapor at the top of the tube.

Since the tube is electrically heated, the heat generation per unit volume is essentially constant. The outside of the tube is assumed to be perfectly insulated. Radial temperature gradients are neglected. The heat transfer coefficients in the vapor film region and in the vapor layer region are taken as constant.

For a heat balance on an element of the tube wall, Kruger obtained

$$\frac{d^2 T}{d\theta^2} - \frac{hr^2}{K_{st}} T = -\frac{hr^2}{K_{st}} T_B - \frac{r^2}{K_{st}} \left[\bar{q}/A - \bar{q}/A_{RAD} \right] \quad (\text{II-45})$$

Equation (II-45) can be applied separately to the two regions of the tube.

In region 1

$$\left. \begin{array}{l} h = h_{LB} \\ T_B = T_s \end{array} \right\} 0 \leq \theta \leq (\pi - \alpha) \quad (\text{II-46a})$$

In region 2

$$\left. \begin{array}{l} h = h_{LV} \\ T_B = T_{vb} \end{array} \right\} (\pi - \alpha) \leq \theta \leq \pi \quad (\text{II-46b})$$

The vapor is considered transparent to radiation from the tube wall. Kruger also assumed that the view factor between the tube wall and the liquid was constant for the values of α/π encountered in the experiments. He also showed that the radiation could be considered constant and evaluated at the mean tube wall temperature without introducing significant error. These assumptions are sufficient to linearize equation (II-45). With these assumptions, the heat transfer by radiation from the tube wall is

$$\bar{q}/A_{RAD} = \epsilon_s \sigma (\bar{T}_w^4 - T_s^4) \quad (\text{II-47})$$

Equation (II-45) can be applied separately to each region as described by (II-46). The boundary conditions to be used are

1. By symmetry

$$\frac{\partial T}{\partial \theta} = 0 \text{ at } \theta = 0 \quad (\text{II-48a})$$

$$\frac{\partial T}{\partial \theta} = 0 \text{ at } \theta = \pi \quad (\text{II-48b})$$

2. For continuity between the two regions

$$T_1 = T_2 \text{ at } \theta = (\pi - \alpha) \quad (\text{II-48c})$$

$$\frac{\partial T_1}{\partial \theta} = \frac{\partial T_2}{\partial \theta} \text{ at } \theta = (\pi - \alpha) \quad (\text{II-48d})$$

For these boundary conditions, Kruger obtained the following equations for the temperature distribution around the tube

$$\frac{T_1 - b_1}{b_2 - b_1} = \frac{1}{\xi} \frac{\cosh a_1 \theta}{\cosh a_1 (\pi - \alpha)} \text{ for } 0 \leq \theta \leq (\pi - \alpha) \quad (\text{II-49a})$$

$$\frac{T_2 - b_2}{b_2 - b_1} = \left(\frac{1}{\xi} - 1 \right) \frac{\cosh a_2 (\pi - \theta)}{\cosh a_2 \alpha} \text{ for } (\pi - \alpha) \leq \theta \leq \pi \quad (\text{II-49b})$$

where

$$\xi = 1 + \frac{a_1}{a_2} \frac{\tanh a_1 (\pi - \alpha)}{\tanh a_2 \alpha} \quad (\text{II-50a})$$

$$a_i = \sqrt{\frac{h_i r^2}{K_{st}}} \quad (\text{II-50b})$$

$$b_i = \left[\frac{1}{h_i} \left(\bar{q}/A - \bar{q}/A_{RAD} \right) + T_{bi} \right] \quad (\text{II-50c})$$

The subscripts refer to the section of the tube wall in which the quantities are to be evaluated. The regions are defined by equation (II-46).

G. Method of Calculation

The temperature distribution in the tube wall can be determined from the equations developed in the theory. Since the properties of the fluid depend on temperature, it is necessary to use an iterative procedure. By assuming a mean tube wall temperature, the fluid properties and the radiation from the tube wall are calculated.

A second difficulty arises because more heat is transferred to the vapor film than to the vapor layer at the top of the tube. By calculating the angle α and the subcooling heat transfer rate, the heat transfer coefficient for the vapor layer can be determined. Based on the assumed mean tube wall temperature, the heat transferred from the tube wall to the vapor layer can be estimated. The corresponding heat that must be transferred from the tube wall at the vapor film region, q/A_T , is then calculated. The heat transfer coefficient for the vapor film can then be determined.

Using the relations for conduction in the tube wall, the tube wall temperature distribution can be calculated for a particular location along the tube. The mean tube wall temperature can then be compared to the assumed value. Since the equations are fairly insensitive to the assumed mean temperature, only a few iterations are required.

Using property values supplied by the manufacturer, a special set of figures was prepared for the groups of properties in the equations. This greatly reduces the time required for performing the calculations. It was necessary to extrapolate

the properties to obtain values at the temperatures encountered in the experiment.

The calculation procedure is:

1. Assume a mean tube wall temperature \bar{T}_W
2. Calculate q/A_{RAD} from (II-47)
3. Calculate q/A_{SCL} from (II-16) and q/A_{SC} from (II-13)
4. Calculate α/π from (II-37)
5. Calculate h_{LV} from (II-41) for a highly subcooled liquid flow, or from (II-44) for a saturated liquid flow.
6. Using the assumed value of \bar{T}_W , estimate the heat transferred to the vapor and calculate the corresponding value of q/A_T .
7. Calculate h_{LB} from (II-26)
8. Calculate a_1 , b_1 , and ξ from (II-50)
9. Calculate T_1 and T_2 from (II-49)
10. Calculate the mean tube wall temperature, \bar{T}_W , and compare it to the assumed value.

Results for these calculations are discussed in Chapter IV, and are shown in Figures 12 through 22 for saturated liquid flows and for highly subcooled liquid flows.

III EXPERIMENTAL PROGRAM

A. Introduction

The object of the experimental program was to determine the relation between tube wall temperature, heat transfer rate, flow rate, liquid subcooling, and fluid properties for film boiling in a horizontal tube. The investigation was limited to the region where the mass flow of vapor is small compared to the total mass flow in the tube.

After making a few minor alterations, the experiments were performed on the apparatus originally designed by Kruger (ref. 12). The equipment is designed for operation with Freon-113 flowing through an electrically heated tube. There are two test sections. The first can be used for visual and photographic observation. A photograph of the stratified flow pattern observed with this test section is shown in Figure 1. The second test section has an electrically heated stainless steel tube instrumented to measure temperatures at the top and bottom of the tube. A series of guard heaters are used on this test section to prevent heat losses to the atmosphere.

B. Description of Apparatus

The apparatus was designed to be used for both visual and quantitative investigations of film boiling. A schematic diagram showing the main components of the equipment is presented

in Figure 2. More detailed schematics of the visual and quantitative test sections are shown in Figures 3 and 4. Photographs of the actual equipment are shown in Figures 5 and 6.

The apparatus consists of two parallel test sections with one circulation system. The circulation system includes a pump, preheater, condenser, degasser, liquid reservoir, pressure and flow control valves, and rotameters for measuring the liquid flow rate.

The preheater has two heat exchangers made from 20 feet of $\frac{1}{2}$ inch copper tubing coiled in a tank. Temperature is controlled by varying the flow of hot and cold water into the tank. A similar heat exchanger is used for the condenser.

A degasser tank was added to the system to insure that no air was dissolved in the Freon-113. This was simply a brass tank surrounded with a water jacket. The tank had sufficient surface area so that air would rise to the top of the tank where it could be bled away. Hot water was circulated through the tank to drive the air out of the solution. Air is less dense than Freon-113 vapor, and rises to the top of the tank. Since the circulation system was sealed, the degasser could be used as a second condenser after all the air had been driven out of the flow.

Two rotameters were connected in parallel to measure the fluid flow. The rotameters were of different capacity to allow more accurate flow measurements.

A pressure gauge is connected to the system to measure the pressure at the test section inlet. A thermocouple was placed at the preheater outlet to measure the fluid temperature at the test section entrance. Another thermocouple was placed at the condenser outlet to insure that all the vapor was being condensed.

An electrically conducting glass tube with an inside diameter of .418 inches was used for the visual test section. The tube is coated with a semitransparent, electrically conducting material. An ammeter was used to measure the current passing through the tube. The tube was heated from a 220 volt power supply.

A stainless steel tube, .403 inch inside diameter and 15 inches long, was used for the quantitative test section. This test section has a high current d.c. power supply which gives the wide range of controlled power input necessary for the tests. In addition to insulation, there is an electrically powered guard heater ring around the tube to minimize heat losses to the atmosphere. The guard heater ring is at a diameter of 2.5 inches around the tube. The space between the tube and guard heater ring is filled with an insulation of known thermal conductivity.

Thermocouples are located at the top and bottom of the tube at six positions along the tube. There are six guard heaters in the guard heater ring and two end guard heaters. Each has independent controls so that the electrical heat input

to each can be adjusted separately. There is a thermocouple in each guard heater so that the losses to the atmosphere can be measured and adjusted. The thermocouples in the guard heater ring are located half way between the top and bottom tube wall thermocouples. The heat losses are minimized by maintaining these guard heaters at a temperature half way between the top and bottom tube wall temperatures.

A continuous recording Honeywell Potentiometer was installed. There are 16 channels on the recorder. By using a switching circuit, the recorder was operated with 32 channels. This reduced the time to record all the data for one run to thirty seconds. It originally required five minutes to record the data for one run with a simple potentiometer.

C. Measurements and Accuracy

All temperature measurements were made with chromel-alumel thermocouples. Thermocouples were installed directly in the flow to measure the temperature of the fluid before it enters the test section and as it leaves the condenser.

The thermocouples in the guard heaters were insulated with ceramic tubing to separate them from the guard heater wires. The thermocouples on the tube were tied over thin mica sheets to prevent any electric contact with the tube. Kruger (ref. 12) showed that, for the heat transfer rate encountered in the experiment, the maximum difference between the inner and outer surfaces of the tube would not exceed 3°F.

The average heat transfer rate per unit surface area of the tube was determined from the following relation for the power input.

$$(\bar{q}/A_s) = \frac{1}{A_s} \left(\rho' \frac{L}{A_c} \right) I^2 \quad (\text{III-1})$$

where A_s is the surface area on the inside of the tube, ρ' the resistivity of the tube, L the length of the tube, A_c the cross sectional area of the tube, and I the current flowing in the tube.

Values for resistivity of stainless steel were obtained from a materials handbook as a function of temperature. For the temperature variations along the tube, encountered in the experiments, the heat transfer rate would vary only a few percent. For this reason, the heat transfer rate was calculated for the value of resistivity at the average tube wall temperature.

The current was measured from the voltage drop across a shunt in the power line. The shunt resistance had been calibrated by the National Bureau of Standards to within 0.1%. The current had a tendency to wander over a period of time. This effect was minimized by installing the recorder to reduce the time required to record all the data for a run.

The voltage drop across the tube was measured by using a resistance bridge. This was used only as a check on the value determined for the heat transfer rate.

The guard heaters were maintained at a temperature between the temperatures measured at the top and bottom of the tube wall.

A temperature difference of 100°F between the tube wall and the guard heater ring represents only a 1% heat loss. Since the guard heaters were easily maintained within 100°F of the tube wall temperature, the heat losses are negligible. The end guard heaters were used to minimize losses along the electrical leads.

Gaskets $1/8$ inch thick were used to separate the electrically heated section from the inlet and outlet lines. These gaskets were also necessary to reduce heat conduction axially along the tube.

Kruger found that the maximum error in the rotameter readings was less than 5% for the range of these tests.

The recorder and associated switching system could cause some error in the temperature and current readings. Tests were made to determine this error, but no error could be detected within the limits of the recorder scale. At lower recorder readings, where the percentage error for a reading is larger due to the number of scale divisions, the readings were checked with the potentiometer for added accuracy.

D. Experimental Technique

Due to limitations in the equipment, it was necessary to use a certain amount of care in operating the apparatus. In order to prevent damage to the test section, a limit of 1000°F was placed on the maximum allowable temperature. For this reason, the test section was heated to the minimum temperature at which stable film boiling could be maintained before the

fluid was started through the test section. For Freon-113 this is approximately 500°F. If the tube was heated while the fluid was flowing, there is a danger of exceeding 1000°F as the boiling process changes from the stable nucleate boiling region to the stable film boiling region.

Before the liquid flow is started, the test section is heated by turning on the guard heaters. The valves on the quantitative test section are closed and the valve opened on the visual test section. The system is then filled with Freon-113 and sealed. The flow is started and bypassed through the visual test section.

While the main test section is being heated to 500°F, there are other operations to perform. The preheater and condensers are put into operation. The preheater is used to heat the liquid to the saturation temperature to drive the air out of the solution. The degasser is also heated and the air is bled away. This procedure is maintained until all the air has been removed from the system.

The main power supply is turned on periodically in order to heat the tube at a faster rate. When the proper temperatures have been reached in the test section and the guard heaters balanced, the main power is turned on and set at the level for the first test. The valves are quickly opened to start the liquid flow in the test section before any overheating can result. The complete starting process takes approximately three hours.

When the run has been started, the preheater and condenser temperatures are adjusted to the proper level. The flow rate and power level are also set to the desired values. When the guard heaters have been balanced and the tube temperatures have reached equilibrium, the data can be recorded. All the data for a run can be recorded in thirty seconds. Approximately twenty minutes are required to reach equilibrium. The experimental conditions can then be changed and the second run started. Another twenty minutes are required to reach equilibrium again.

In operating the visual test section, the flow is bypassed through the quantitative test section. The proper temperature level to establish film boiling in the visual section is obtained by a trial and error process. Only a few minutes are required to heat the visual test section to the proper temperature since the 220 volt power supply is used.

If the flow is started before the proper temperature level is reached, the film boiling will change over to nucleate boiling and immediately cool the tube. In the visual test section, it was observed that there is a sharp interface between the nucleate and film boiling regions. This interface can be seen in Figure 1. The interface gradually moves downstream if the heat losses are high. This effect can also be observed in the main test section, when the tube wall temperatures are too low. When the interface travels downstream beyond a thermocouple location, the temperature drops rapidly back to a value typical of the nucleate region.

E. Data Recorded

All experiments were conducted with Freon-113 as the test fluid. The pressure in the test section is essentially constant for a given run. The pressures recorded in the test section ranged from 3 to 7.5 psig. for the entire test series. This corresponds to liquid saturation temperatures of 125°F to 141°F.

The subcooling ranged from 6°F to 52°F for the tests.

The heat transfer rates per unit area ranged from 12,200 Btu/hr-ft² to 19,600 Btu/hr-ft².

The runs were made for two values of the liquid velocity at the entrance to the test section. These were 1.23 ft/sec. and 1.85 ft/sec.

The temperature of the liquid at the condenser outlet was recorded to be certain that all the vapor had been condensed.

Guard heater temperatures were recorded. These were always balanced at a value between the top and bottom tube wall temperatures.

Temperatures at the top and bottom of the tube wall were measured at six positions along the length of the tube. These points were: $x = 0.083$ ft., $x = 0.271$ ft., $x = 0.50$ ft., $x = 0.75$ ft., $x = 0.978$ ft., and $x = 1.17$ ft. Because of the high end losses near the outlet of the heated section, only the first five values are reported.

The important data is recorded in the Table of Experimental Results. These results are also shown in Figures 12 through 22.

IV RESULTS AND CONCLUSIONS

A. Discussion

The results of the experimental investigation are shown in Figures 12 through 22. Calculations from the analysis are also shown for saturated liquid flows and for highly subcooled liquid flows. In these figures the temperature difference is plotted as a function of the distance from the tube inlet. The temperature difference is tube wall temperature minus fluid saturation temperature.

Three basic differences were observed in the tube wall temperature distribution when the liquid was subcooled. They are:

1. Near the tube inlet, lower tube wall temperatures were observed with a subcooled liquid flow than those measured for a comparable saturated liquid flow.
2. Near the tube outlet, higher tube wall temperatures were observed with a subcooled liquid flow than those measured at any location along the tube for a comparable saturated liquid flow.
3. The difference between top and bottom tube wall temperature increased significantly with a subcooled liquid flow.

All these effects are shown in Figures 12, 13 and 14. In these figures the heat transfer rate and flow rate are constant and the amount of subcooling is the variable.

Figures 15 and 16 show that as the subcooling is increased, the maximum tube wall temperature continues to rise. The average tube temperatures are shown in these figures for different amounts of subcooling. The heat transfer rate and flow rate are again the same for all runs.

A better correlation of the data is obtained by holding the subcooling and flow rate constant while the heat transfer rate is varied. Figures 17 through 22 show that this type of correlation does not exhibit the temperature profile crossover effect illustrated in Figures 12 through 16. For clarity, the mean tube wall temperature is used in these figures.

When the temperature profile crossover effect was first observed, some changes were made in the apparatus. First, a degasser was added to make certain that the results were not affected by air dissolved in the Freon-113. A pressure control was added so that the test section pressure could be held constant for both saturated and subcooled liquid flows. These changes had no effect on the observed temperature profile crossover.

The heat transfer rates were also carefully observed to be certain that there were no significant differences between saturated and subcooled runs. Runs were made where the liquid was gradually subcooled and the changing temperature profiles were continuously observed during this process.

Observation in the visual test section showed that no basic change occurred in the stratified flow as a result of subcooling.

An explanation of the effect can be obtained from the three basic differences observed with subcooling. First, higher tube wall temperatures indicate that the overall average heat transfer coefficient near the outlet of the tube is lower when the liquid is subcooled. The overall average heat transfer coefficient would include radiation, convection into the vapor layer and convection into the vapor film.

At the inlet, the film covers most of the tube, and convection into the vapor film is the most important method of heat transfer. With subcooling the observed tube wall temperatures were lower near the tube inlet. Since subcooling reduces the vapor in the film, the film heat transfer coefficient would be expected to increase. This would result in a lower tube wall temperature with subcooling. Therefore, the cross-over effect does not appear to be the result of any unusual effects taking place in the vapor film.

There is no reason to believe the heat transferred from the wall by radiation would be significantly affected by subcooling the liquid flow. The only other method of heat transfer is convection into the vapor layer.

The effect of the heat transferred into the vapor increases along the tube. This is due to the larger flow area occupied by the vapor. Since the increase in tube wall temperatures for subcooled flows occurs downstream from the inlet, it seems reasonable to suspect that the heat transferred to the vapor layer is reduced by subcooling.

The increased difference between top and bottom tube wall temperatures means that the ratio of heat transferred to the vapor layer to heat transferred to the vapor film must be increasing with subcooling. Since the film heat transfer coefficient would be higher with subcooling, this effect would be expected. However, the difference was much larger than that observed in the saturated case. This also indicates that subcooling reduces the heat transferred to the vapor.

Since the temperatures at the outlet of the tube with subcooled flow greatly exceed the maximum temperature anywhere on a tube with saturated flow, the effect of subcooling on the heat transferred to the vapor layer must be very great. To account for this effect requires more than a small reduction in the vapor layer heat transfer coefficient.

When the vapor layer starts to grow near the tube inlet, the boundary layers developing at the tube wall and at the horizontal interface are probably laminar. However, as the vapor Reynolds number increases due to vapor formation, the boundary layers could become turbulent.

The rate of vapor formation is greater when the liquid flow is saturated. This means the disturbances in the vapor layer are greater than would occur with a subcooled liquid flow. Greater disturbances in the boundary layer can cause a transition to turbulent flow at lower vapor Reynolds numbers. Under these conditions, the vapor layer would become turbulent at much lower vapor Reynolds numbers.

Subcooling could result in condensation at the horizontal liquid-vapor interface. The boundary layer could remain stable to very high vapor Reynolds numbers under these conditions.

Heat transfer coefficients in the vapor layer would be many times higher for turbulent flow than for laminar flow at the same Reynolds number. This effect is large enough to account for the much higher tube wall temperatures observed with subcooled flow.

In order to predict the tube wall temperature distribution, it would be necessary to develop a criterion to determine the heat transfer coefficient in the region of transition from laminar to turbulent flow. Such a relation must include the effect of subcooling on transition. No method has been developed as yet to predict this transition.

Since a criterion was not developed to predict transition, only the limiting cases can be determined from the theory. With saturated liquid flow, the transition would take place close to the tube inlet. It was assumed that the vapor layer was turbulent for a saturated liquid flow.

With high subcooling, 50°F for these experiments, the vapor layer was assumed to remain laminar over the entire length of the tube.

It was necessary to assume a bulk temperature in the vapor layer to make these calculations. An analysis was made to

determine a value for the bulk temperature by considering the conditions at the interface. This analysis showed that the bulk temperature was approximately half way between the tube wall temperature and saturation temperature for both subcooled and saturated liquid flow. This value was used in the calculations.

The bulk temperature effect, although in the right direction, was not large enough to cause the increased temperatures with subcooling. Since the predominant effect appears to be the transition from laminar to turbulent flow, the effect of changes in the bulk temperature in the vapor layer were neglected. To determine temperature distribution for intermediate amounts of subcooling, this effect might have to be included in the analysis.

The model chosen for subcooling was discussed completely in the theoretical section. The effects of other assumptions in the theory were discussed in detail by Kruger (ref. 12).

The results of the analysis made with these assumptions are shown in Figures 12 through 22. For the limiting cases, the analysis shows good agreement with the experiment.

The calculations compare favorably with experimental results with respect to:

1. Temperature level,
2. Temperature distribution around the tube,
3. Rate of change of temperature along the tube, and
4. Relative level of temperatures along the tube for subcooled flows with respect to saturated flows.

B. Summary of Results and Conclusions

1. Experimental results are presented for film boiling with subcooling of the liquid flow for Freon-113 flowing inside a horizontal tube.

2. A theoretical model was developed which explains the effects observed with subcooled liquid flow. Calculations are presented for saturated and highly subcooled liquid flows which appear to represent, with a certain degree of accuracy, the results observed in the experiments. The analysis cannot accurately predict the effects of intermediate values of subcooling.

3. Both the theory and experimental investigations were limited to the region in which the mass flow of vapor is small compared to the total mass flow.

4. The region in which the theoretical model applies was not determined.

5. Visual observation confirmed many of the basic assumptions made in the flow model.

6. Near the tube inlet subcooling the liquid decreases the tube wall temperature, while it increases the tube wall temperature downstream.

45,

NOMENCLATURE

English Symbols

A	= Area
a_1, b_1	= Non-dimensional parameters
b	= Thickness of the vapor film
C	= Constant
C_p	= Specific heat at constant pressure
D	= Diameter
D_e	= Equivalent diameter
f	= Friction factor
g	= Acceleration of gravity
h	= Heat transfer coefficient
I	= Electric current
K	= Thermal conductivity
K_s	= Thermal conductivity of the steel tube
L	= Length of the tube
P	= Pressure
q	= Heat transfer rate
(q/A)	= Heat transfer rate per unit area
(\bar{q}/A)	= Mean heat transfer rate per unit area
r	= Radius
T	= Temperature
t	= Thickness of the tube wall
V	= Velocity
V_0	= Velocity of the liquid at the test section inlet

- w = Mass flow rate
 x = Distance from the tube inlet
 X_m = Non-dimensional tube length-flow rate factor
 y = Distance from interface to the tube wall in the vapor film

Greek Symbols

- α = Interface angle shown in Figure 7
 β' = Experimentally determined coefficient related to velocity at liquid vapor interface in film region
 γ = Averaging factor for the local boiling heat transfer coefficient
 ϵ_s = Emissivity of the tube surface
 θ = Angle from the bottom of the tube shown in Figure 7
 λ = Latent heat of the liquid
 χ = Average heat content of the vapor
 μ = Viscosity
 ξ = Non-dimensional number
 ρ = Density
 ρ' = Electrical resistivity
 σ = Stefan-Boltsman constant

Subscripts

- B = Refers to a temperature in tube wall conduction equations
 c = Convection
 co = Convection in the absence of radiation

f = Temperature of liquid at tube inlet
i = Horizontal liquid-vapor interface
L = Liquid
LB = Local conditions in the boiling region
LV = Local conditions in the vapor region
r = Radial
RAD = Radiation
s = Saturation temperature
S = Refers to surface area
sc = Refers to subcooling
T = Total
V = Vapor
Vb = Refers to vapor layer at top of tube
VF = Refers to vapor film region
W = Conditions at the tube wall
1 = Evaluated in the region
2 = Evaluated in the region

45.
BIBLIOGRAPHY

1. Rohsenow, W. M., Heat Transfer - A Symposium, University of Michigan, 1952, pp. 101
2. Westwater, J. W., "Boiling of Liquids", Advances in Chemical Engineering, Academic Press, Inc., New York, 1956
3. Berenson, P. J., "Transition Boiling Heat Transfer from a Horizontal Surface", M.I.T. Division of Sponsored Research Technical Report No. 17, 1960
4. Bradfield, W. S., "Plane Laminar Forced Convection Film Boiling with Subcooling", Convair Scientific Research Laboratory Research Note 35, 1960
5. Cess, R. D. and Sparrow, E. M., "Film Boiling in a Forced Convection Boundary Layer Flow", A.S.M.E. Paper No. 60-WA-148, 1960
6. Bromley, L. A., "Heat Transfer in Stable Film Boiling", United States Atomic Energy Commission, AECD-2295, 1948
7. Bromley, L. A., LeRoy, N. R. and Robbers, J. A., "Heat Transfer in Forced Convection Film Boiling", Industrial and Engineering Chemistry, vol. 45, 1954, pp. 2639
8. Hsu, Y. Y., and Westwater, J. W., "Film Boiling from Vertical Tubes", Presented at the A.S.M.E.-A.I.Ch.E. Joint Heat Transfer Conference, 1957
9. Hsu, Y. Y., and Westwater, "Approximate Theory for Film Boiling on Vertical Surfaces", Presented at the Third National Heat Transfer Conference, A.S.M.E.-A.I.Ch.E., 1959

10. Graham, R. W., Hendricks, R. C., Hsu, Y. Y. and Friedman, R., "Experimental Heat Transfer and Pressure Drop of Film Boiling Liquid Hydrogen Flowing through a Heated Tube", Presented at the 1960 Cryogenic Engineering Conference.
11. von Glahn, V. H. and Lewis, J. P., "Nucleate and Film Boiling Studies with Liquid Hydrogen", Advances in Cryogenic Engineering, vol. 5, 1960
12. Kruger, R. A., "Film Boiling on the Inside of Horizontal Tubes in Forced Convection", M.I.T., Department of Mechanical Engineering, June, 1961
13. Motte, E. I. and Bromley, L. A., "Film Boiling of Flowing Subcooled Liquids", Industrial and Engineering Chemistry, vol. 49, 1957, pp. 1921
14. Schneider, P. J., Conduction Heat Transfer, Addison - Wesley Publishing Company, Inc., Massachusetts, 1955, pp. 240
15. Eckert, E. R. G. and Drake, R. M., Heat and Mass Transfer, 2nd Edition, McGraw-Hill Book Company, Inc., New York, 1959
16. McAdams, W. H., Heat Transmission, 3rd Edition, McGraw-Hill Book Company, Inc., New York, 1954
17. Bromley, L. A., Brodkey, R. S. and Fishman, Norman, "Heat Transfer in Condensation, Part II, Effect of Heat Capacity on Condensate", Industrial and Engineering Chemistry, vol. 44, 1952, pp. 2966

APPENDIX A

Velocity Profile in the Vapor Film

A parabolic velocity profile was assumed in the vapor film. The general form of the equation is

$$\frac{V}{\bar{V}} = C_1 + C_2 \frac{y}{b} + C_3 \left(\frac{y}{b}\right)^2 \quad (\text{A-1})$$

where \bar{V} is the average vapor velocity in the film, y is the distance from the interface to the tube wall, and b is the film thickness.

The velocity, V , at the tube wall must be zero.

$$V = 0 \quad \text{at } y = b \quad (\text{A-2})$$

The average velocity must satisfy the condition

$$\int_0^1 \frac{V}{\bar{V}} d\left(\frac{y}{b}\right) = 1 \quad (\text{A-3})$$

A third condition can be obtained for the total shearing stresses on the vapor

$$\tau_{wT} = \mu_v \left[\left(\frac{dV}{dy}\right)_{y=0} - \left(\frac{dV}{dy}\right)_{y=b} \right] \quad (\text{A-4})$$

The constants in equation (A-1) can be determined from the boundary condition given by (A-2), (A-3), and (A-4). The equation that results is

$$\frac{V}{\bar{V}} = 2\left(1 - \frac{y}{b}\right) - \frac{b\tau_{wT}}{6\mu_v\bar{V}} \left(1 - 4\frac{y}{b} + 3\left(\frac{y}{b}\right)^2\right) \quad (\text{A-5})$$

The limits on the shearing stress can be determined. If the liquid at the interface is rigid, then

$$\left(\frac{dV}{dy}\right)_{y=0} = \left(\frac{dV}{dy}\right)_{y=b} \quad (\text{A-6})$$

and the maximum shearing stress is

$$\tau_{WT \max} = \frac{12 \mu_v \bar{V}}{b} \quad (\text{A-7})$$

face

$$\left(\frac{dV}{dy} \right)_{y=0} = 0 \quad (\text{A-8})$$

and the minimum shearing stress is

$$\tau_{WT} = \frac{3 \mu_v \bar{V}}{b} \quad (\text{A-9})$$

The coefficient β' is defined as

$$\beta' \equiv \frac{\tau_{WT} b}{2 \mu_v \bar{V}} \quad (\text{A-10})$$

The limits on β' are

$$\frac{3}{2} \leq \beta' \leq 6 \quad (\text{A-11})$$

Kruger (ref. 12) determined that the best experimental correlation is obtained when $\beta' = 1.4$.

Substituting (A-10) into (A-5) yields

$$\frac{V}{\bar{V}} = 2 \left(1 - \frac{y}{b} \right) - \frac{1}{3} \beta'^3 \left(1 - 4 \frac{y}{b} + 3 \left(\frac{y}{b} \right)^2 \right) \quad (\text{A-12})$$

The velocity at the liquid-vapor interface is

$$V = \left(2 - \frac{1}{3} \beta'^3 \right) \bar{V} \quad (\text{A-13})$$

TABLE OF EXPERIMENTAL RESULTS

The double subscripts in the following table indicate the location of the tube wall temperature measurements in the following manner.

A. The first subscript refers to the position of the thermocouple along the tube as shown below.

Subscript	x - ft.
1	0.083
2	0.27
3	0.50
4	0.75
5	0.98

B. The second subscript refers to the position of the thermocouple around the tube as shown below.

b - Bottom of tube wall

t - Top of tube wall

m - Arithmetic mean of top and bottom tube wall
temperature

TABLE OF EXPERIMENTAL RESULTS

<u>Run No.</u>	<u>1</u>	<u>2</u>	<u>3</u>	<u>4</u>	<u>5</u>	<u>6</u>
V_o - ft./sec.	1.85	1.85	1.85	1.85	1.85	1.85
I - amps.	253	247	247	253	253	256
$(\overline{q/A})$ - Btu./hr.ft. ²	13680	13100	13150	13800	13820	14150
P - psig.	6.5	5.5	5.5	5.5	5.5	4.0
T_s - °F	139	136	136	136	136	131
T_f - °F	126	119	117	117	116	103
$(T_s - T_f)$ - °F	13	17	19	19	20	28
$(T_{1b} - T_s)$ - °F	458	457	472	475	479	455
$(T_{1t} - T_s)$ - °F	510	526	526	530	532	505
$(T_{1m} - T_s)$ - °F	484	492	499	503	506	480
$(T_{2b} - T_s)$ - °F	540	530	547	547	552	531
$(T_{2t} - T_s)$ - °F	596	608	608	612	612	591
$(T_{2m} - T_s)$ - °F	568	569	578	580	582	561
$(T_{3b} - T_s)$ - °F	544	539	556	560	565	567
$(T_{3t} - T_s)$ - °F	600	618	618	622	624	634
$(T_{3m} - T_s)$ - °F	572	579	587	591	595	601
$(T_{4b} - T_s)$ - °F	540	539	556	560	565	578
$(T_{4t} - T_s)$ - °F	598	622	622	629	633	657
$(T_{4m} - T_s)$ - °F	569	581	589	595	599	618
$(T_{5b} - T_s)$ - °F	544	549	565	573	577	587
$(T_{5t} - T_s)$ - °F	598	631	631	639	641	668
$(T_{5m} - T_s)$ - °F	571	590	598	606	609	628

(Con't)

TABLE OF EXPERIMENTAL RESULTS

<u>Run No.</u>	<u>7</u>	<u>8</u>	<u>9</u>	<u>10</u>	<u>11</u>	<u>12</u>
V_o - ft./sec.	1.85	1.85	1.85	1.85	1.85	1.85
I - amps.	265	271	274	268	265	268
(q/A) - Btu./hr.ft. ²	15420	16200	16620	15900	15400	15900
P - psig.	6.5	6.0	6.0	6.0	6.0	5.0
T_s - °F	139	137	137	137	137	134
T_f - °F	122	117	117	117	117	104
$(T_s - T_f)$ - °F	17	20	20	20	20	30
$(T_{1b} - T_s)$ - °F	519	536	551	546	512	532
$(T_{1t} - T_s)$ - °F	579	594	611	604	572	592
$(T_{1m} - T_s)$ - °F	549	565	581	575	542	562
$(T_{2b} - T_s)$ - °F	600	611	626	617	585	593
$(T_{2t} - T_s)$ - °F	660	670	687	679	645	656
$(T_{2m} - T_s)$ - °F	630	641	657	648	615	625
$(T_{3b} - T_s)$ - °F	605	617	630	623	594	622
$(T_{3t} - T_s)$ - °F	664	679	691	685	653	694
$(T_{3m} - T_s)$ - °F	635	648	661	654	624	658
$(T_{4b} - T_s)$ - °F	605	617	630	623	598	639
$(T_{4t} - T_s)$ - °F	664	687	700	691	666	720
$(T_{4m} - T_s)$ - °F	635	652	665	657	632	680
$(T_{5b} - T_s)$ - °F	605	625	641	632	611	650
$(T_{5t} - T_s)$ - °F	664	691	704	700	679	732
$(T_{5m} - T_s)$ - °F	635	658	673	666	645	691

(Con't)

TABLE OF EXPERIMENTAL RESULTS

<u>Run No.</u>	<u>13</u>	<u>14</u>	<u>15</u>	<u>16</u>	<u>17</u>	<u>18</u>
V_o - ft./sec.	1.85	1.85	1.85	1.85	1.85	1.85
I - amps.	265	265	277	280	283	277
$\overline{(q/A)}$ - Btu./hr.ft. ²	15500	15420	17270	17820	18150	17300
P - psig.	4.5	3.5	6.0	5.0	5.0	5.0
T_s - °F	133	130	137	134	134	134
T_f - °F	102	84	112	102	98	100
$(T_s - T_f)$ - °F	31	46	25	32	36	34
$(T_{1b} - T_s)$ - °F	516	485	598	605	597	584
$(T_{1t} - T_s)$ - °F	574	536	657	665	656	648
$(T_{1m} - T_s)$ - °F	545	511	628	635	627	616
$(T_{2b} - T_s)$ - °F	585	566	662	656	650	643
$(T_{2t} - T_s)$ - °F	644	635	725	720	716	707
$(T_{2m} - T_s)$ - °F	615	601	694	688	683	675
$(T_{3b} - T_s)$ - °F	623	609	666	686	688	682
$(T_{3t} - T_s)$ - °F	696	681	729	760	764	758
$(T_{3m} - T_s)$ - °F	660	645	698	723	726	720
$(T_{4b} - T_s)$ - °F	636	626	666	701	701	695
$(T_{4t} - T_s)$ - °F	720	711	743	791	791	787
$(T_{4m} - T_s)$ - °F	678	669	705	746	746	741
$(T_{5b} - T_s)$ - °F	644	643	683	715	713	711
$(T_{5t} - T_s)$ - °F	729	732	755	800	805	796
$(T_{5m} - T_s)$ - °F	687	688	719	758	759	754

(Con't)

TABLE OF EXPERIMENTAL RESULTS

<u>Run No.</u>	<u>19</u>	<u>20</u>	<u>21</u>	<u>22</u>	<u>23</u>	<u>24</u>
V_o - ft./sec.	1.85	1.85	1.85	1.85	1.85	1.85
I - amps.	277	295	295	250	262	265
$\frac{q}{A}$ - Btu./hr.ft. ²	17070	19780	19600	13220	14880	15290
P - psig.	3.0	7.5	7.5	6.0	6.5	6.5
T_s - °F	127	141	141	137	138	138
T_f - °F	77	121	121	123	123	123
$(T_s - T_f)$ - °F	50	20	20	14	15	15
$(T_{1b} - T_s)$ - °F	509	619	603	460	503	507
$(T_{1t} - T_s)$ - °F	552	679	658	512	563	567
$(T_{1m} - T_s)$ - °F	531	649	631	486	533	537
$(T_{2b} - T_s)$ - °F	608	698	687	514	563	567
$(T_{2t} - T_s)$ - °F	680	764	753	576	627	635
$(T_{2m} - T_s)$ - °F	644	731	720	545	595	601
$(T_{3b} - T_s)$ - °F	659	692	675	506	563	567
$(T_{3t} - T_s)$ - °F	739	746	725	564	627	635
$(T_{3m} - T_s)$ - °F	699	719	700	535	595	601
$(T_{4b} - T_s)$ - °F	684	687	666	512	576	580
$(T_{4t} - T_s)$ - °F	773	746	721	568	635	644
$(T_{4m} - T_s)$ - °F	729	717	694	540	606	612
$(T_{5b} - T_s)$ - °F	706	683	658	521	582	588
$(T_{5t} - T_s)$ - °F	798	742	713	572	640	646
$(T_{5m} - T_s)$ - °F	752	713	686	547	611	617

(Con't)

TABLE OF EXPERIMENTAL RESULTS

<u>Run No.</u>	<u>25</u>	<u>26</u>	<u>27</u>	<u>28</u>	<u>29</u>	<u>30</u>
V_o - ft./sec.	1.85	1.85	1.85	1.85	1.85	1.85
I - amps.	265	271	265	271	241	289
$\overline{(q/A)}$ - Btu./hr.ft. ²	15210	16020	15250	16210	12220	18800
P - psig.	6.5	6.5	6.5	6.5	3.0	3.0
T_s - °F	138	138	138	138	125	125
T_f - °F	108	104	102	123	110	73
$(T_s - T_f)$ - °F	30	34	36	15	15	52
$(T_{1b} - T_s)$ - °F	455	473	446	539	433	529
$(T_{1t} - T_s)$ - °F	528	528	503	597	485	593
$(T_{1m} - T_s)$ - °F	492	501	475	568	459	561
$(T_{2b} - T_s)$ - °F	520	533	524	595	503	644
$(T_{2t} - T_s)$ - °F	593	610	593	661	556	716
$(T_{2m} - T_s)$ - °F	557	572	559	628	530	680
$(T_{3b} - T_s)$ - °F	554	576	563	608	511	682
$(T_{3t} - T_s)$ - °F	635	656	644	673	556	758
$(T_{3m} - T_s)$ - °F	595	616	604	641	534	720
$(T_{4b} - T_s)$ - °F	588	610	597	622	515	712
$(T_{4t} - T_s)$ - °F	669	690	682	690	571	800
$(T_{4m} - T_s)$ - °F	629	650	640	656	543	756
$(T_{5b} - T_s)$ - °F	610	631	618	637	535	746
$(T_{5t} - T_s)$ - °F	694	716	707	703	593	839
$(T_{5m} - T_s)$ - °F	652	674	663	670	564	793

(Con't)

TABLE OF EXPERIMENTAL RESULTS

<u>Run No.</u>	<u>31</u>	<u>32</u>	<u>33</u>
V_o - ft./sec.	1.85	1.23	1.23
I - amps.	289	283	283
$\overline{(q/A)}$ - Btu./hr.ft. ²	19050	18000	17660
P - psig.	3.0	5.5	5.5
T_s - °F	125	136	136
T_f - °F	102	130	90
$(T_s - T_f)$ - °F	23	6	46
$(T_{1b} - T_s)$ - °F	593	586	461
$(T_{1t} - T_s)$ - °F	657	637	509
$(T_{1m} - T_s)$ - °F	625	612	485
$(T_{2b} - T_s)$ - °F	686	684	556
$(T_{2t} - T_s)$ - °F	750	751	635
$(T_{2m} - T_s)$ - °F	718	718	596
$(T_{3b} - T_s)$ - °F	720	692	603
$(T_{3t} - T_s)$ - °F	784	751	686
$(T_{3m} - T_s)$ - °F	752	722	645
$(T_{4b} - T_s)$ - °F	741	671	650
$(T_{4t} - T_s)$ - °F	822	730	747
$(T_{4m} - T_s)$ - °F	782	701	699
$(T_{5b} - T_s)$ - °F	767	646	701
$(T_{5t} - T_s)$ - °F	847	701	803
$(T_{5m} - T_s)$ - °F	807	674	752



Figure 1 - Film boiling of Freon-113 in a horizontal tube with $V_0 = 1.85$ ft/sec. The flow is from left to right.

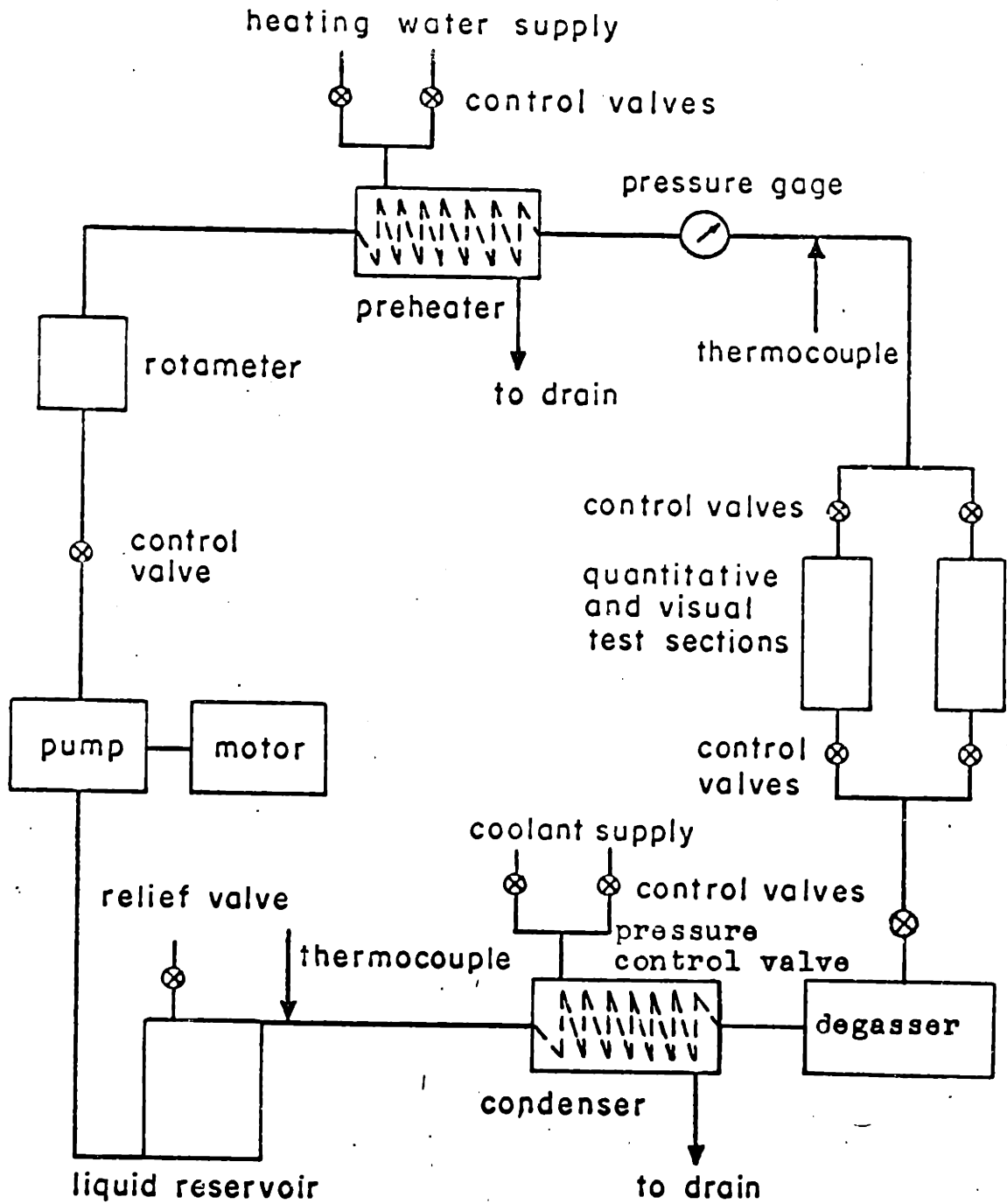
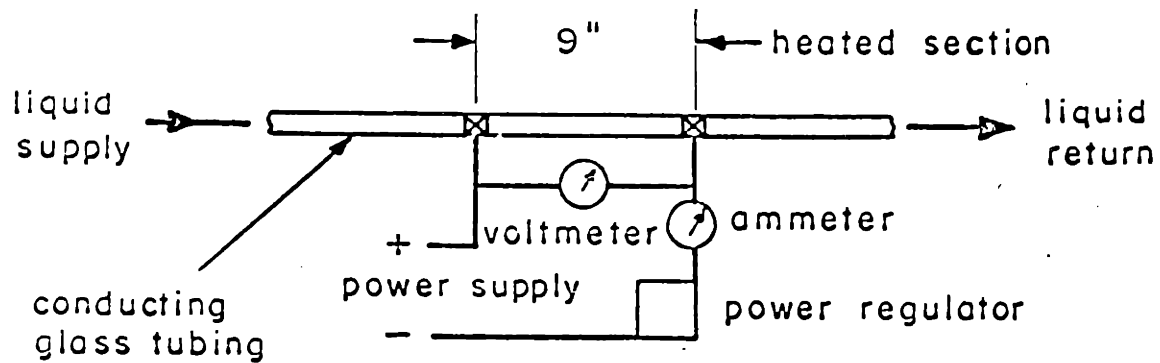


FIG. 2 SCHEMATIC DIAGRAM OF THE CIRCULATION SYSTEM



Tube I. D. = 0.418 inches, L = 48 inches

Fig. 3 SCHEMATIC DIAGRAM OF THE VISUAL TEST SECTION

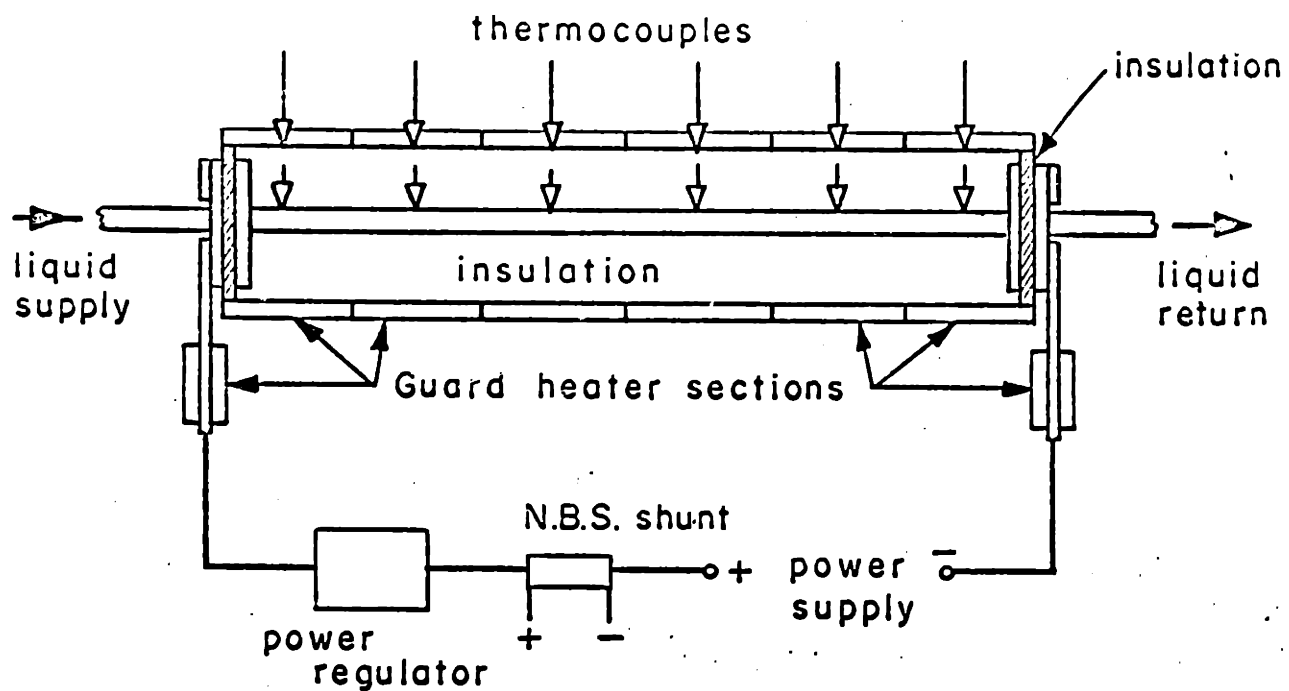


FIG. 4 SCHEMATIC DIAGRAM OF THE QUANTITATIVE TEST SECTION

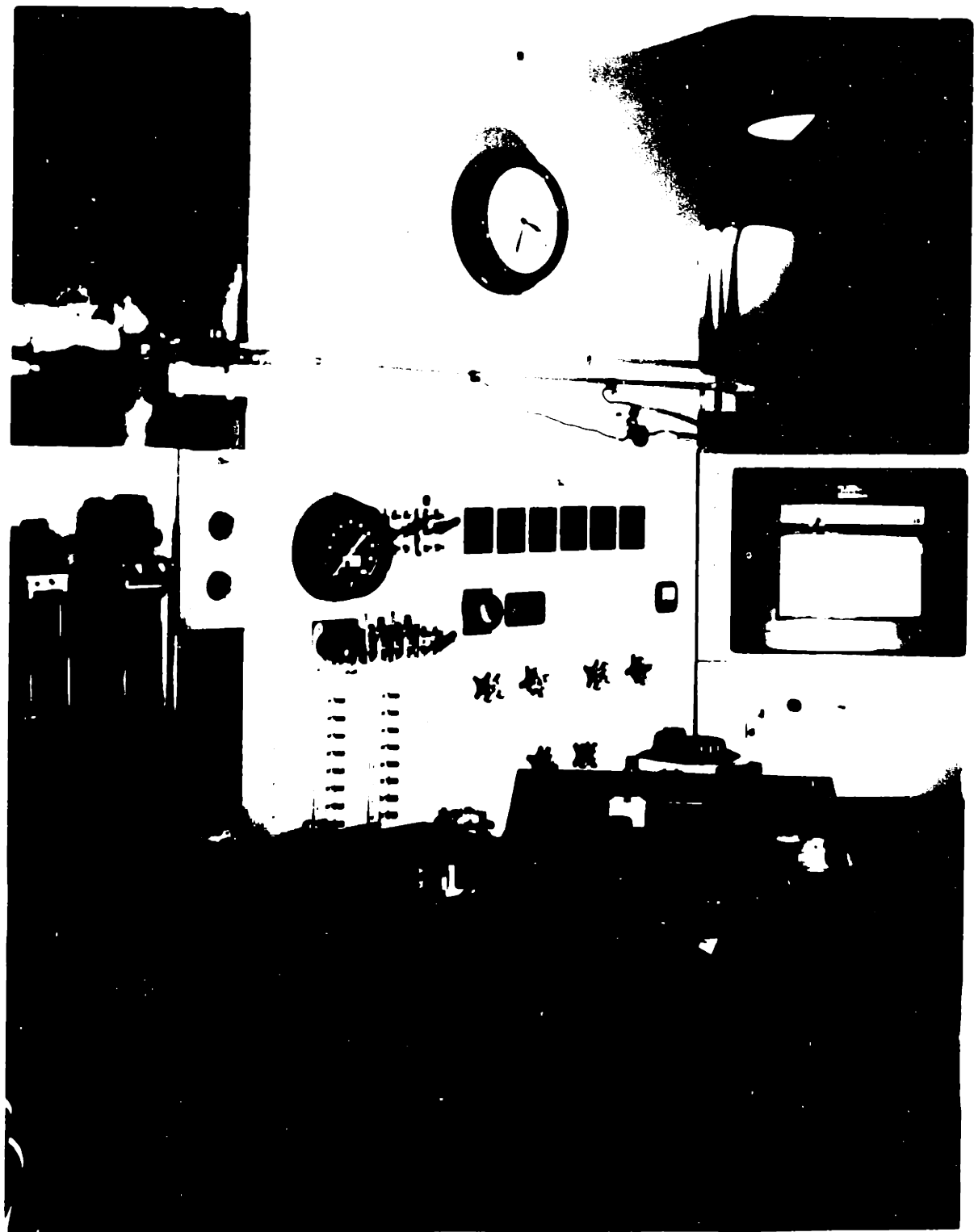


Figure 5 - Apparatus control panel and the visual test section

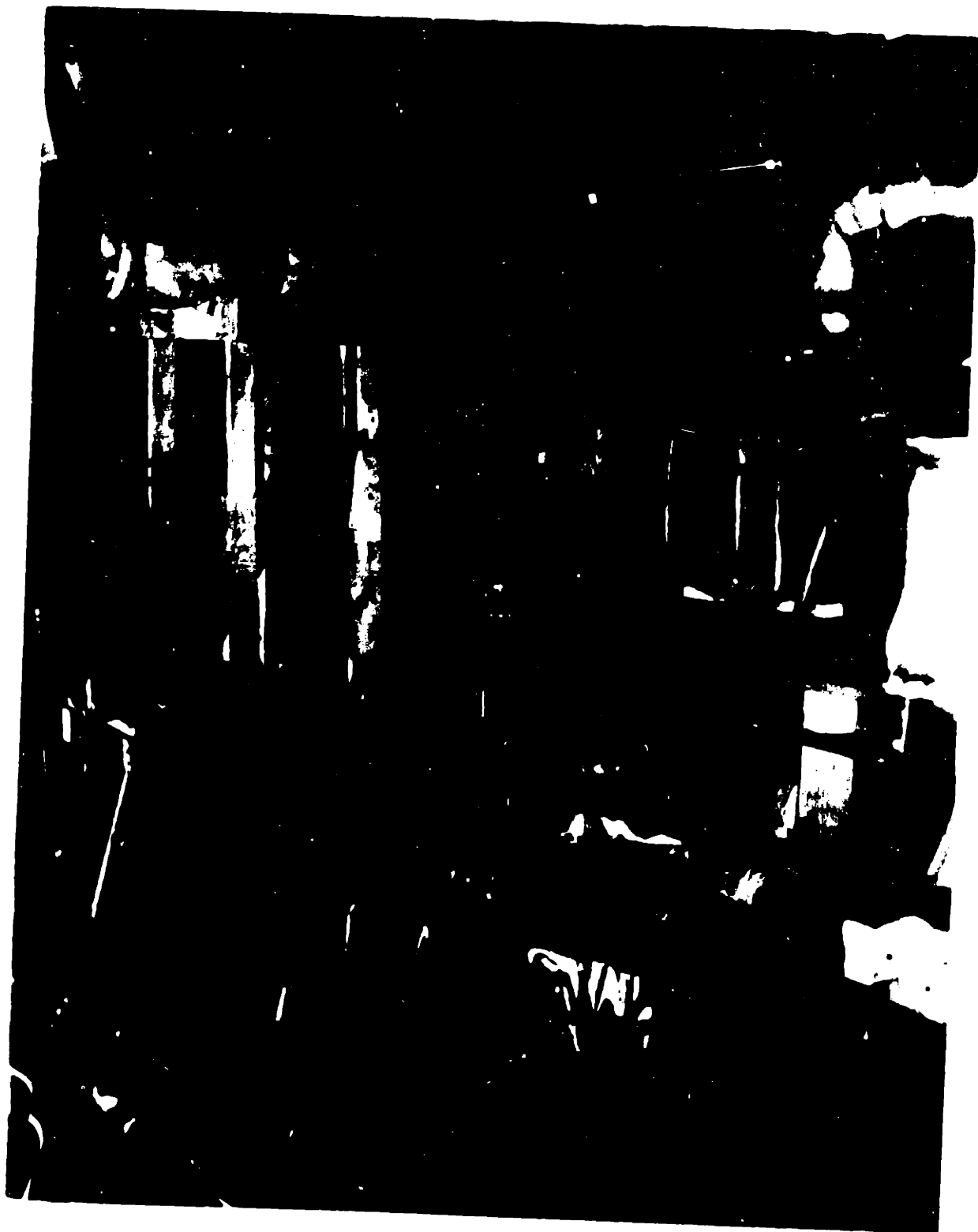


Figure 6 - Quantitative test section and parts
of the control and circulation systems.

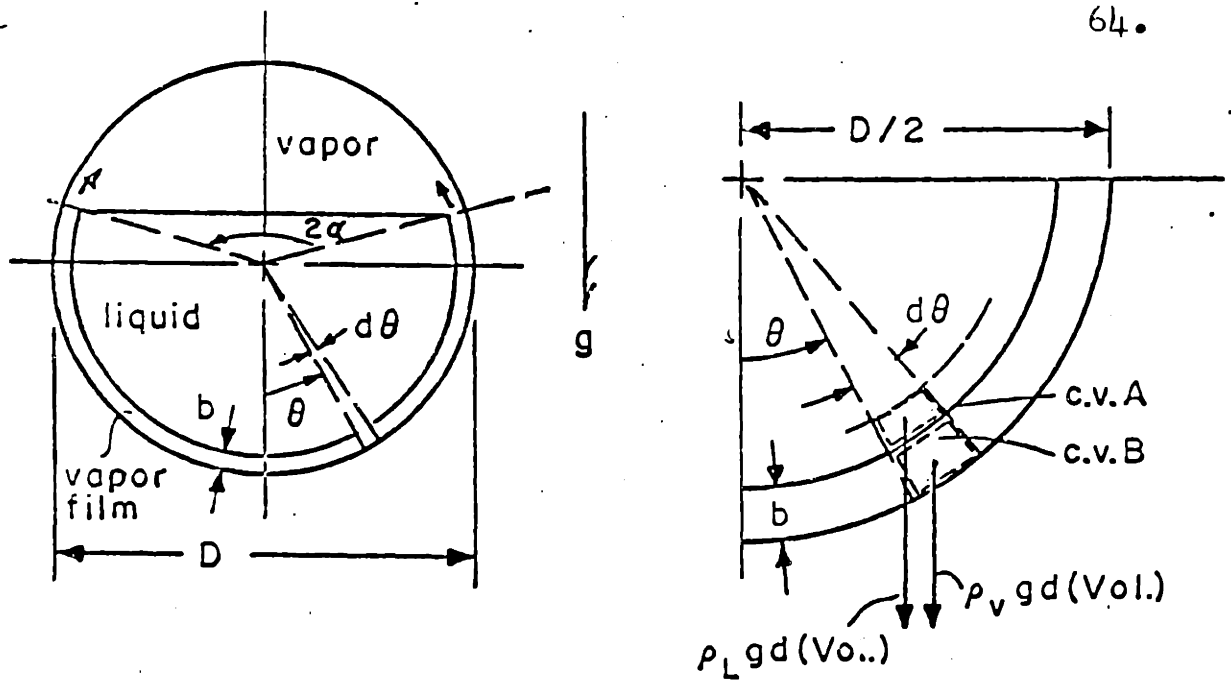


FIG. 7 CROSS SECTION OF IDEALIZED FLOW MODEL

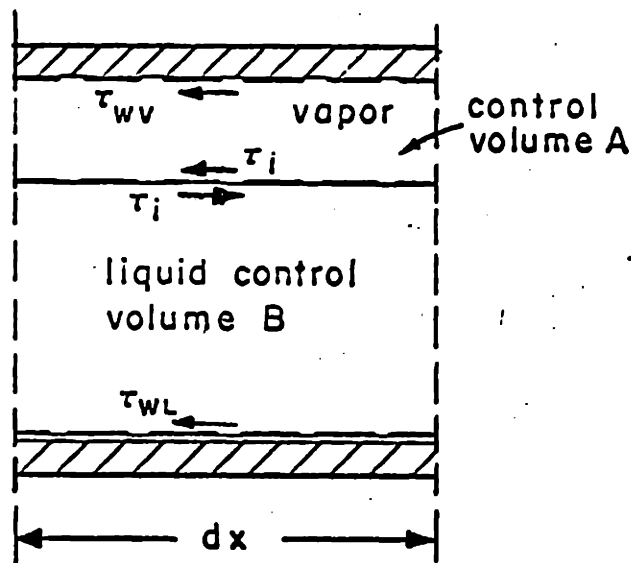


FIG. 8 GEOMETRY FOR MOMENTUM ANALYSIS

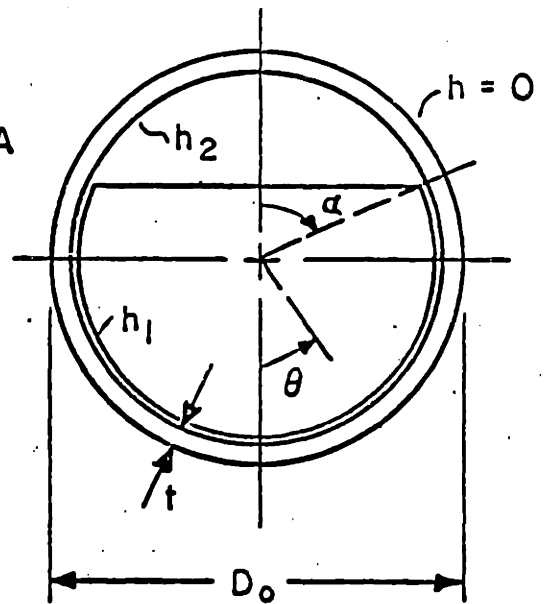


FIG. 9 GEOMETRY FOR CONDUCTION ANALYSIS

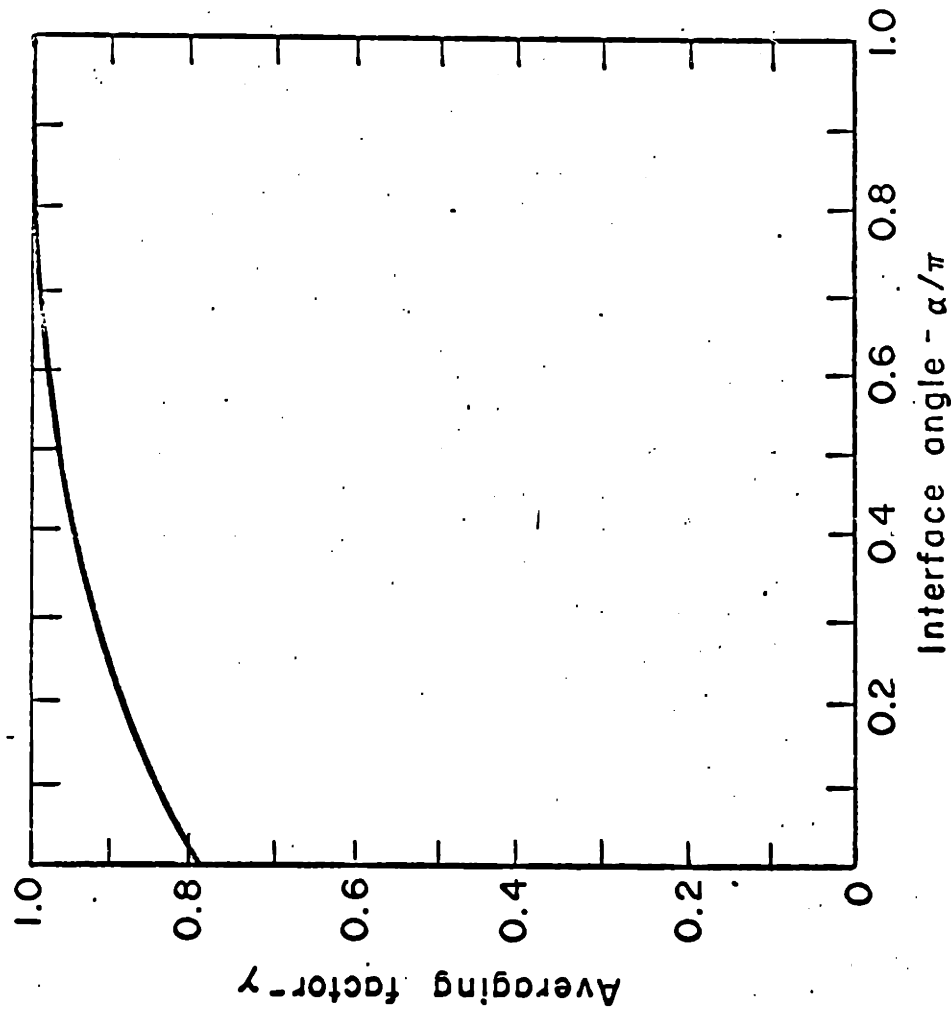


FIG. 10 BOILING HEAT TRANSFER COEFFICIENT MULTIPLIER, γ , vs. α/π

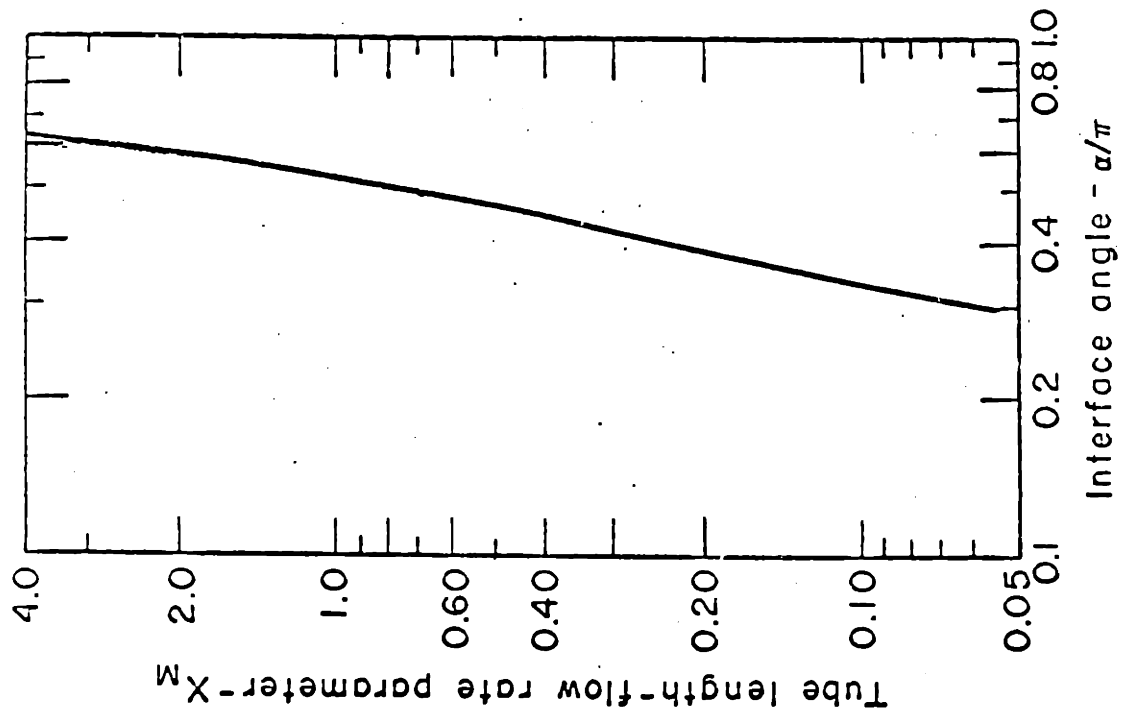


FIG. 11 TUBE LENGTH - FLOW RATE PARAMETER vs. α/π

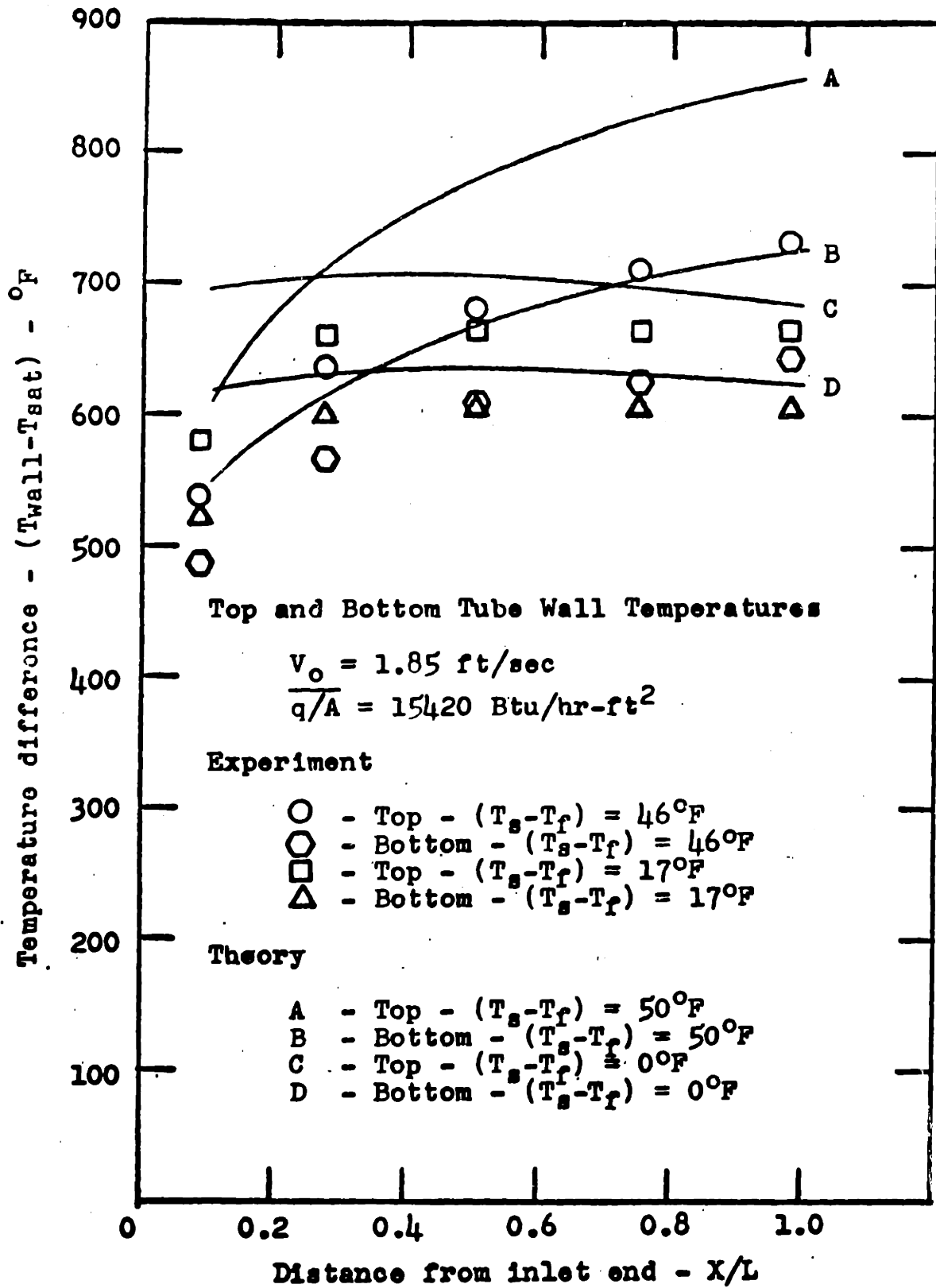


FIG. 12 TEMPERATURE DISTRIBUTION WITH X/L

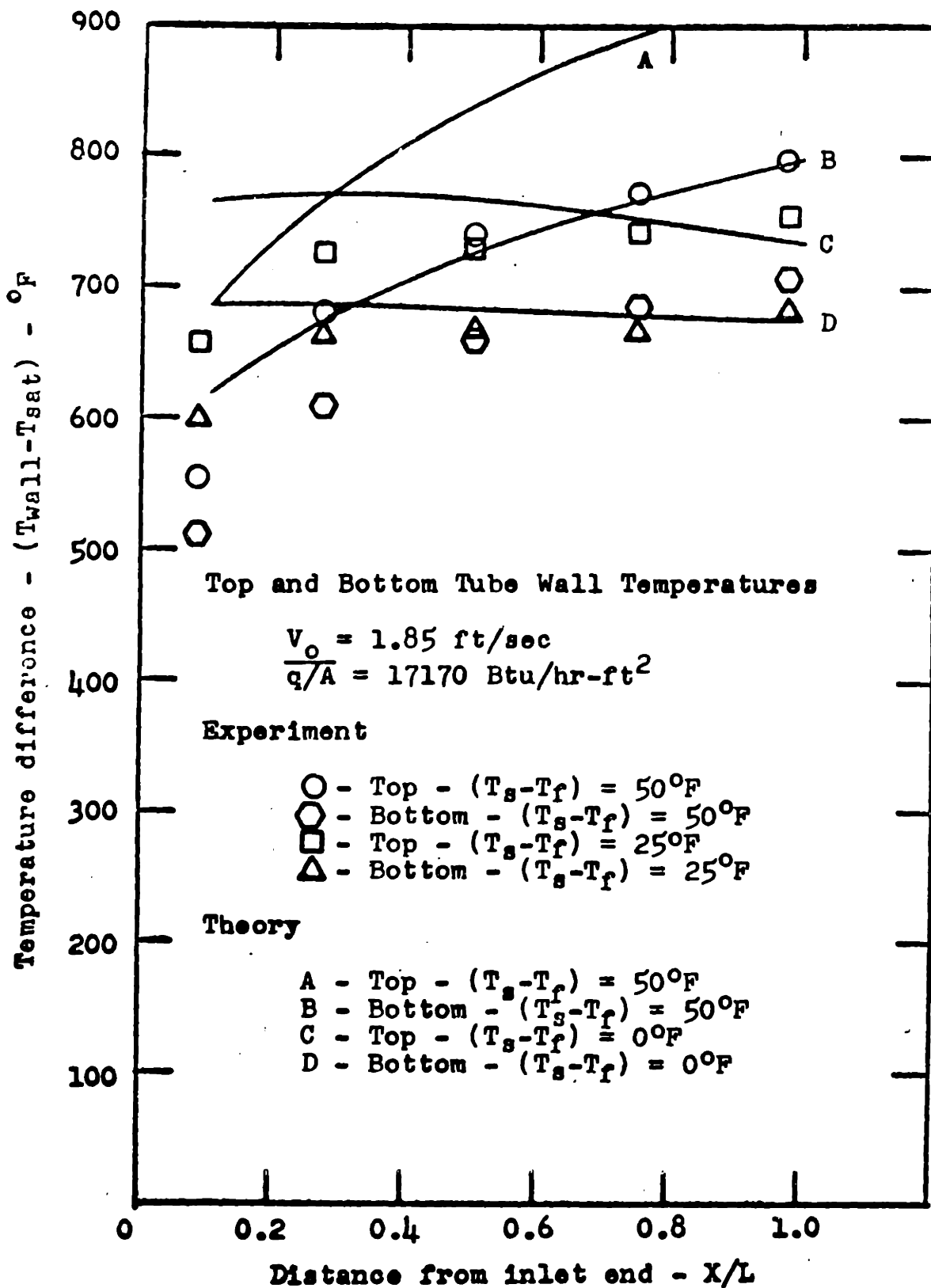


FIG. 13 TEMPERATURE DISTRIBUTION WITH X/L

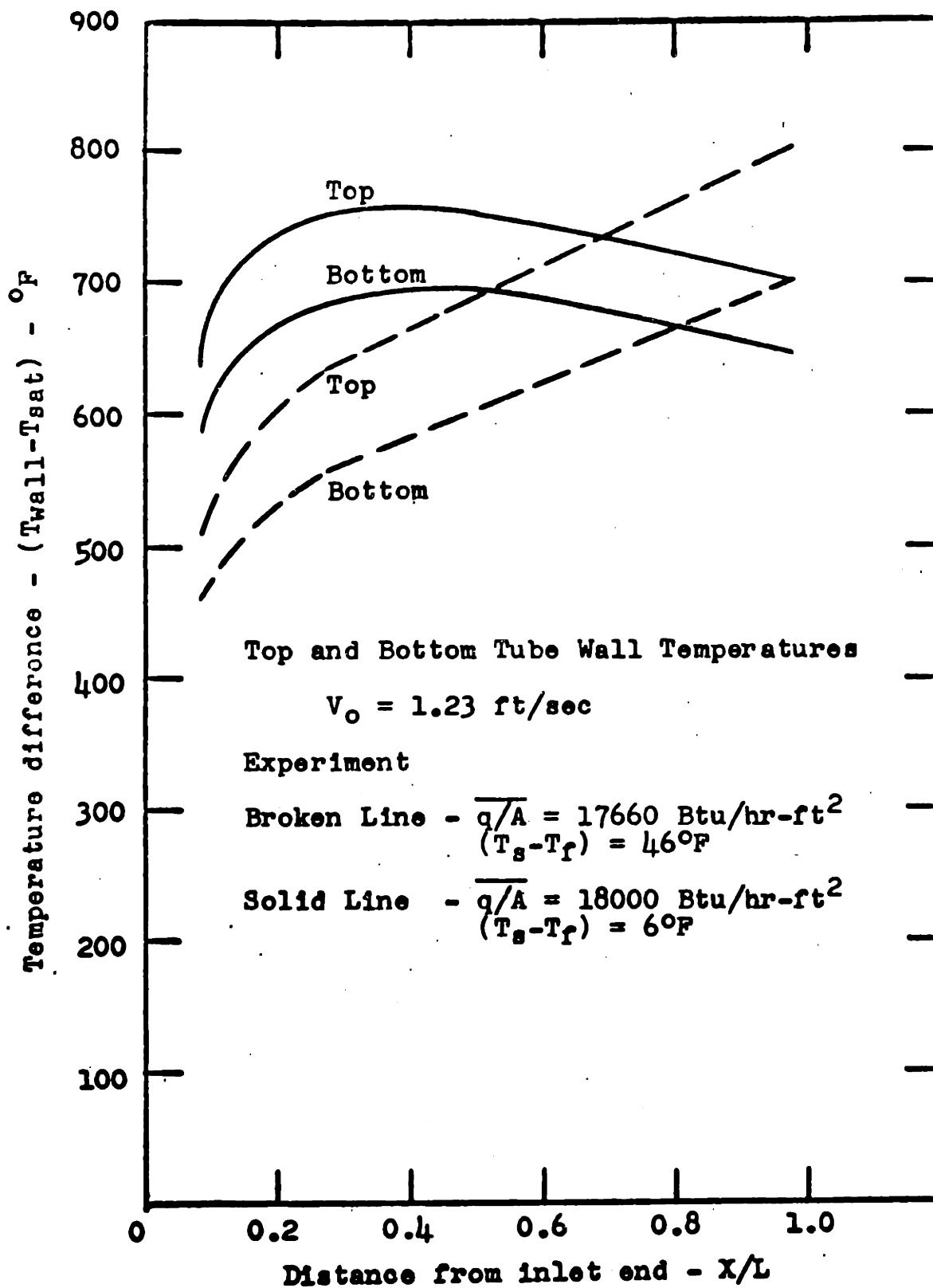


FIG. 14 TEMPERATURE DISTRIBUTION WITH X/L

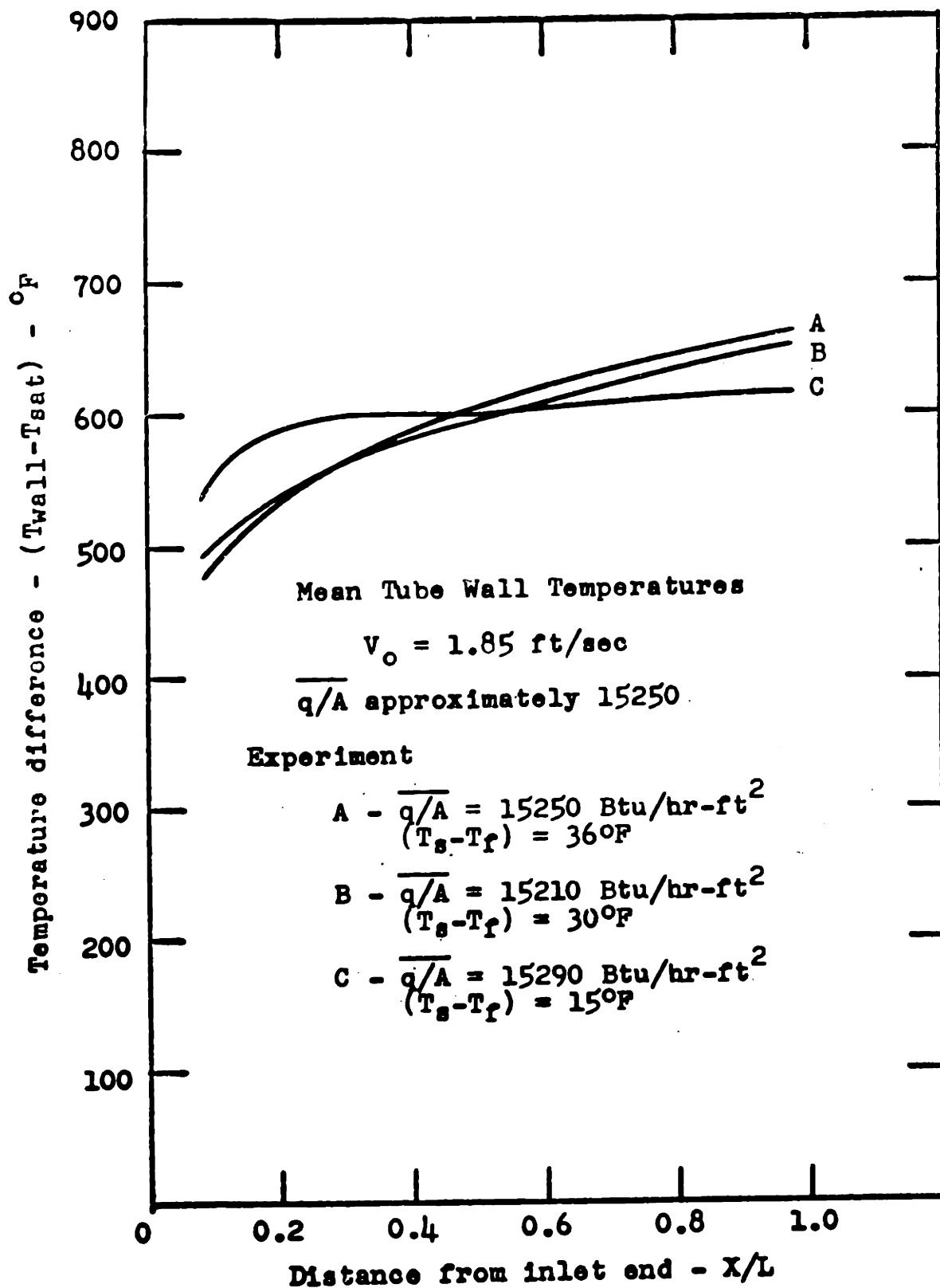


FIG. 15 TEMPERATURE DISTRIBUTION WITH X/L

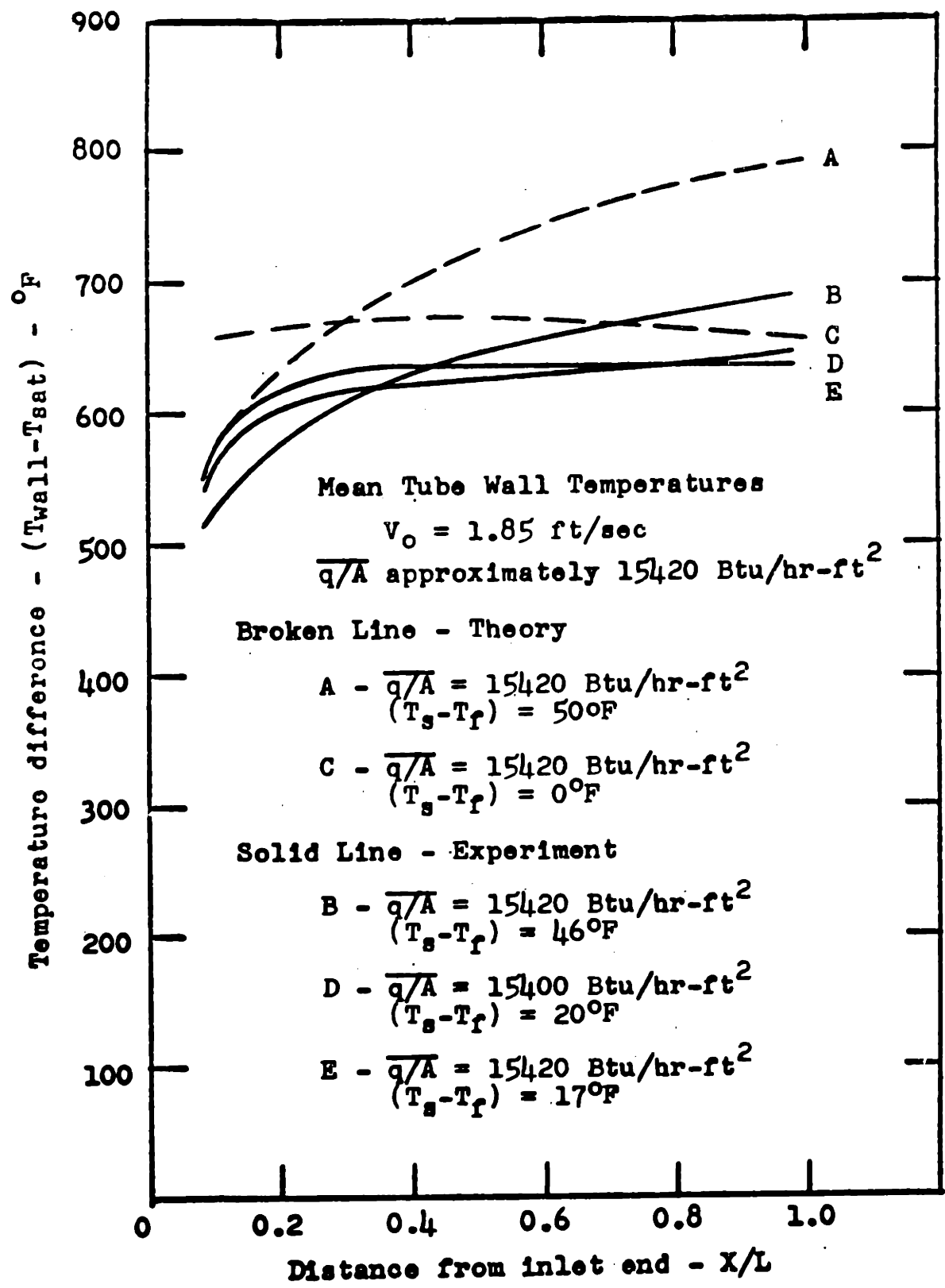


FIG. 16 TEMPERATURE DISTRIBUTION WITH X/L

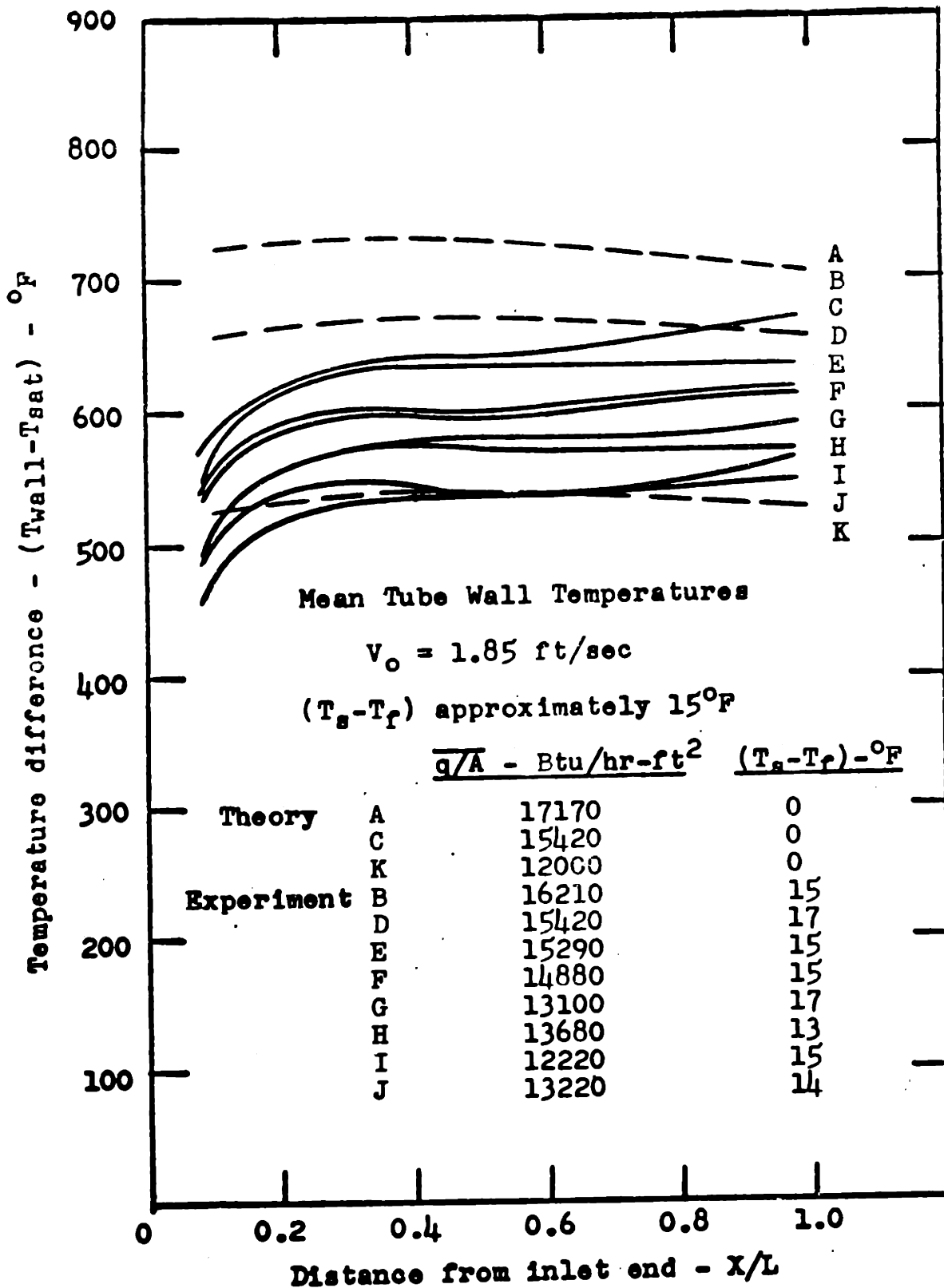
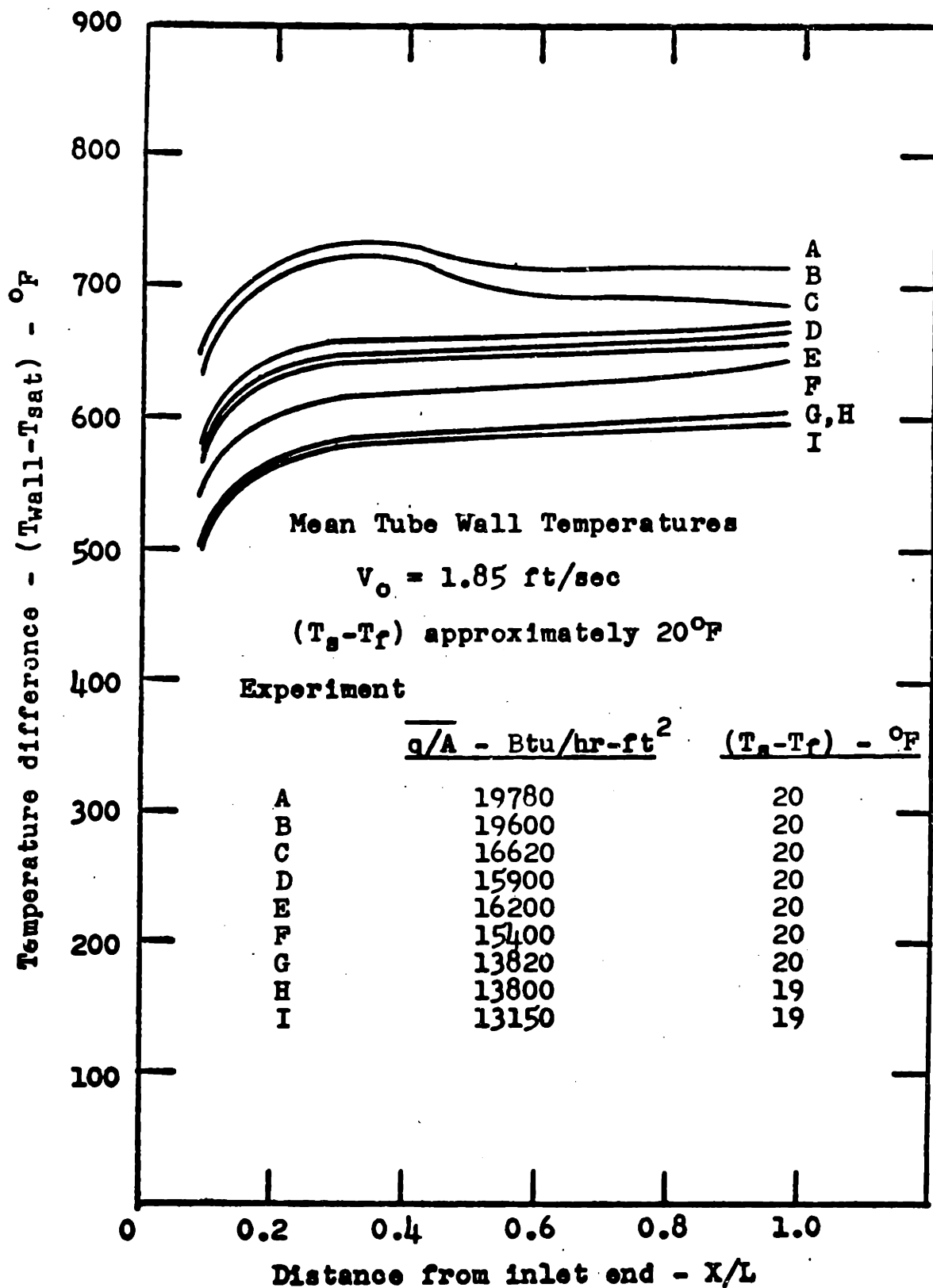


FIG. 17 TEMPERATURE DISTRIBUTION WITH X/L

FIG. 18 TEMPERATURE DISTRIBUTION WITH X/L

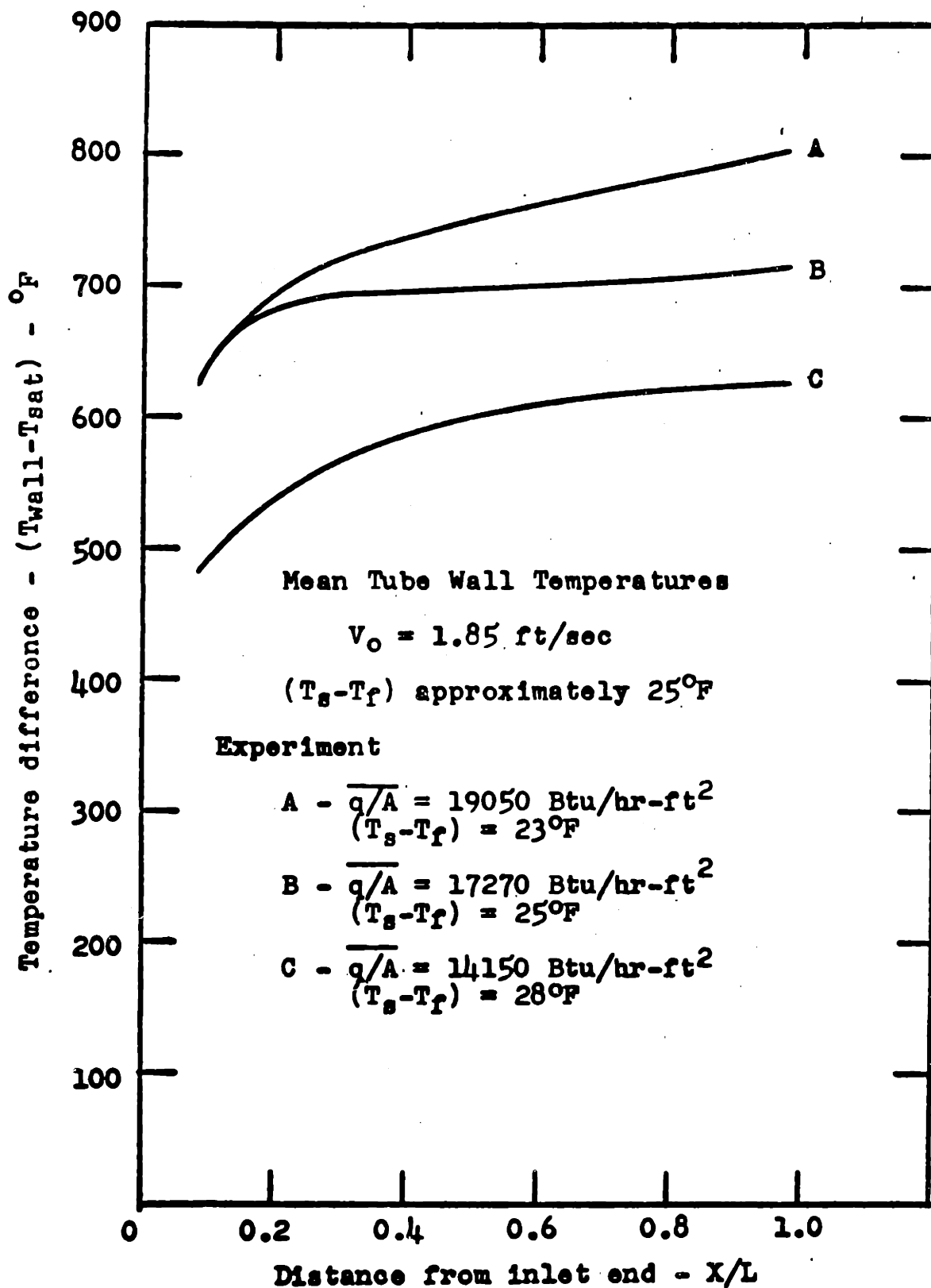


FIG. 19 TEMPERATURE DISTRIBUTION WITH X/L

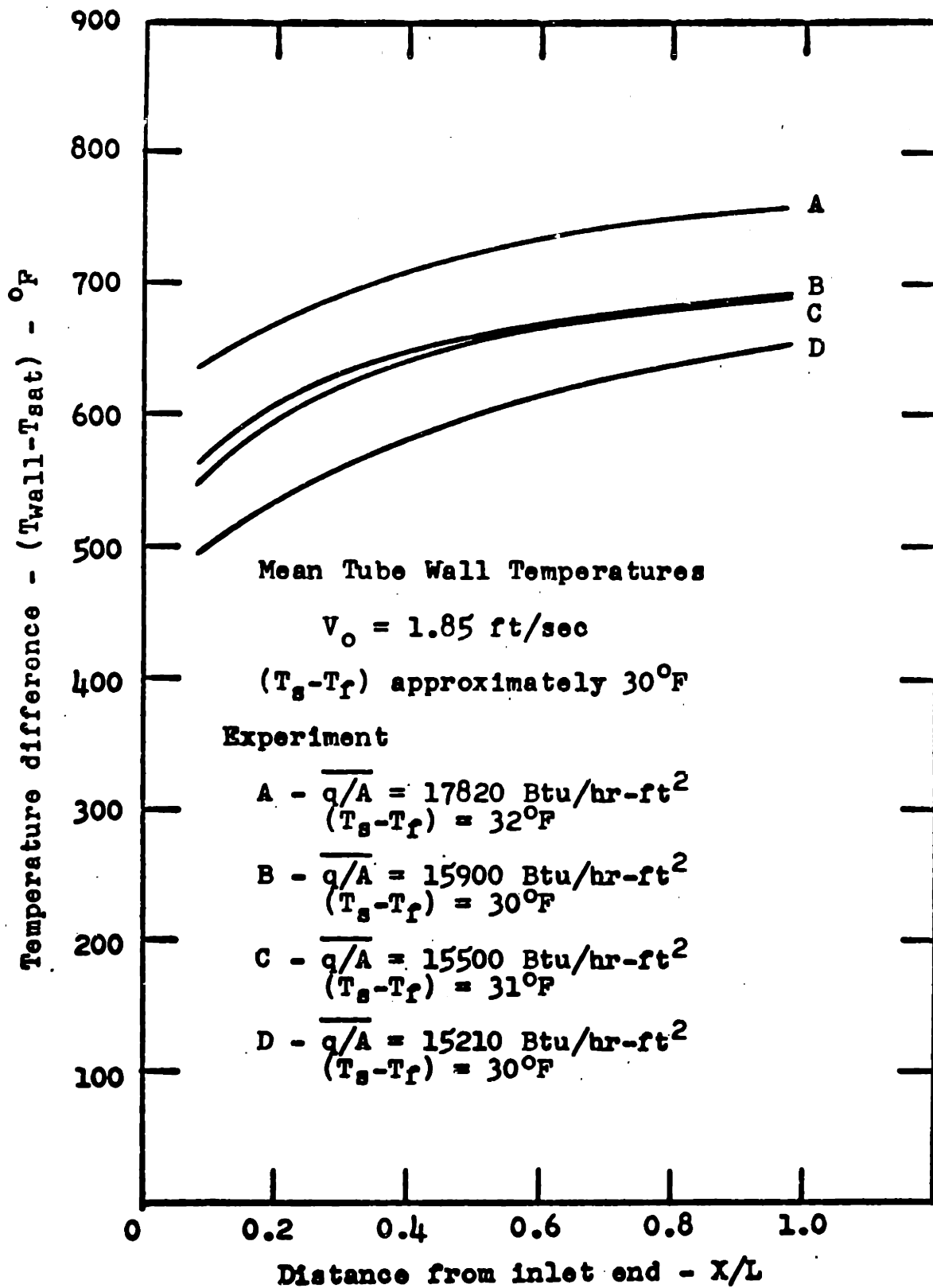


FIG. 20 TEMPERATURE DISTRIBUTION WITH X/L

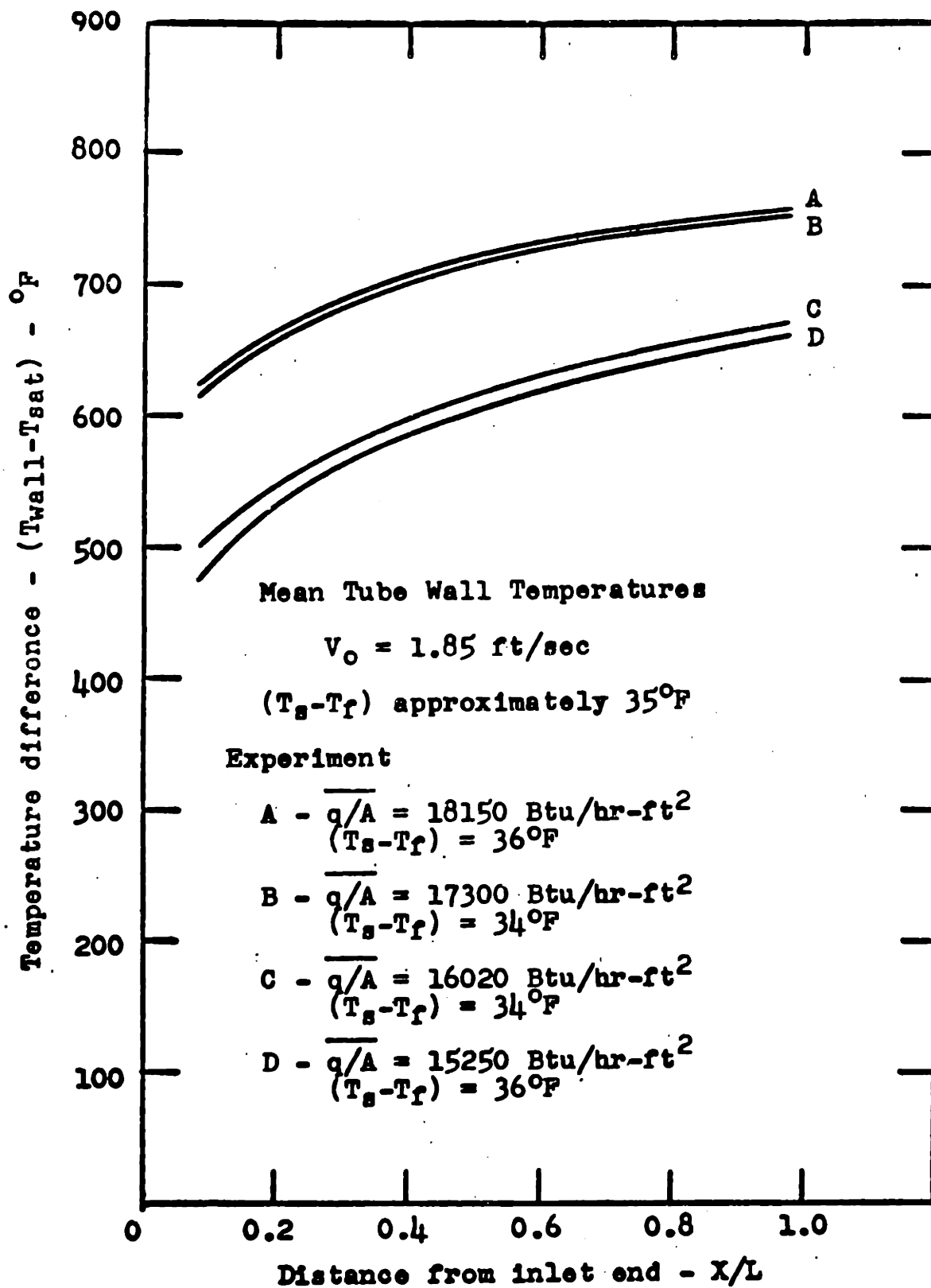


FIG. 21 TEMPERATURE DISTRIBUTION WITH X/L

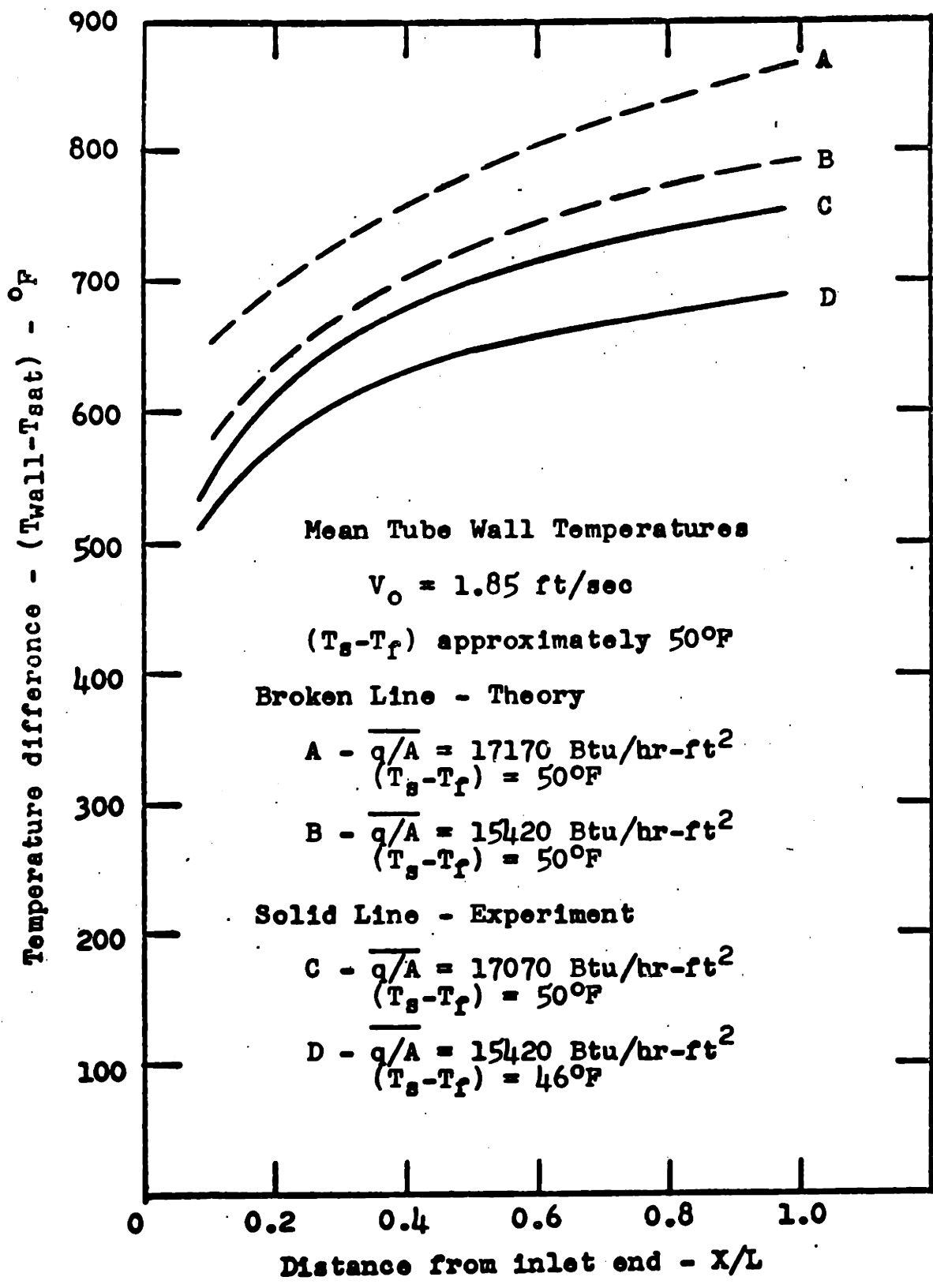


FIG. 22 TEMPERATURE DISTRIBUTION WITH X/L